

Dear editor,

The authors are very thankful and grateful to the two referees who accepted to evaluate the work presented in the submitted manuscript and for their valuable remarks.

Answers to Referee #1 (G. Martinelli) comments:

Values displayed in table 6 are dated back to November 1992 so they are old values. This is the main reason why they are considered high comparatively to what is expected to be found nowadays. In fact, at present times, tritium figures have fallen lower than 5 TU in precipitation measured in the northern part of the country.

Where and when the rain sample was collected:

The value of 16 TU in precipitation was collected from Ouargla itself (from the National Agency for Water Resources (ANRH) station).

The value of 16 TU seems to be high but we can note the following remarks:

We are in an arid area (desert) where precipitation is very scarce and irregular. Precipitation takes place in the form of sudden thunderstorms in an unsaturated atmosphere and a great part of this precipitation evaporates back into the moisture unsaturated atmosphere sometimes during many cycles. Consequently, an enrichment in tritium happens because when water evaporates back, the lightest fractions (isotopes) are the ones that evaporate first causing an enrichment in Tritium in the remaining fraction. The 16 TU value would thus correspond then to a rainy event that had happened during the same sampling period (Nov. 1992). It's the only available value and it's not a weighted mean for a long period of time. It's the most representative value for that region and for that time. Unfortunately, all the other stations (Algiers, Ankara, and Tenerife) are subject to a completely different climatic regime and beside the fact that they have more recent values, can absolutely not be used for our case. Therefore all the assumptions based on recent tritium rain values do not apply to this study.

Unfortunately due to a technical problem at that time, no deuterium values were made available for those samples

Depleted contents in O-18 and low tritium concentrations for phreatic waters fit well the mixing scheme and confirm the contribution from the older and deeper CI/CT groundwaters. The affected areas were clearly identified in the field and correspond to locations that are subject to a recycling and a return of irrigation waters whose origin are CI/CT boreholes. Moreover, the mixing that is clearly brought to light by the Cl vs. O-18 diagrams (Fig. 15 & 16) could partly derive from an ascending drainage from the deep and confined CI aquifer (exhibiting depleted homogenous O-18 contents & very low tritium), a vertical leakage that is favoured by the Anguid El-biod highly faulted area (geological argument).

Answers to Referee #2 (Anonymous) comments:

1- The bullets that are used in the manuscript will be reduced as much as possible especially with regard to the inverse modeling section.

We assume that the relationship between ^{18}O and Cl data obtained in 1996 is stable with time, which is a logical assumption as times of transfer from CI to both CT and Phr are very long. Considering both ^{18}O and Cl data, CI, CT and Phr data populations can be categorized. The CI and CT do not show appreciable ^{18}O variations, and can be considered as a single population. The Phr samples consist however of different populations: Pole I, with $\delta^{18}\text{O}$ values close to -8, and small Cl concentrations, more specifically less than 35 mmol.l⁻¹; Pole II, with $\delta^{18}\text{O}$ values larger than 3, and very large Cl concentrations, more specifically larger than 4000 mmol.l⁻¹; intermediate Phr samples result from mixing between poles I and II (mixing line in Fig. 13, mixing curve in Fig. 14) and from evaporation of pole I (evaporation line in Fig. 14).

2- The literature review will be expanded to include more references of recently published papers such as those suggested (Dai & Sampers, 2004) and a couple of others.

In the present study, new data were collected in order to characterize the hydrochemical and the isotopic composition of the major aquifers in Ouargla's region. They also aimed at identifying the origin of the mineralization and water-rock interactions that occur along the flow. New possibilities offered by progress in geochemical simulations were used. More specifically, the inverse modeling of chemical reactions allows us to select the best conceptual model for the interpretation of the geochemical evolution of the Ouargla aquifer. The stepwise inversion strategy involves designing a list of the scenarios that includes the most plausible combinations of geochemical processes, solving scenarios in a stepwise manner, and selecting the scenario that provides the best conceptual geochemical model (Dai et al., 2006). Inverse modeling with Phreeqc 3.0 was used to quantitatively assess the influence of the processes that explain the acquisition of solutes for the different aquifers: dissolution, precipitation, mixing and ion exchange. This results in constraints on mass balances as well as on the exchange of matter between aquifers.

3- All geochemical data that was measured is presented in the tables. As the authors used PhreeqC, the methodology is already constrained by its use and the mineral that are known and defined by the geological and lithological features of the region of interest has done the rest in the selection of the data to be used

The Inverse modeling involves designing a list of the scenarios that includes the most plausible combinations of geochemical processes. For example, the way to identify whether calcite dissolution/precipitation is relevant or not consists of solving the inverse problem under two alternate scenarios: (1) considering a geochemical system in which calcite is present, and (2) considering a geochemical system without calcite. After solving the two scenarios, it is usually possible to

select the better result as the solution of the inverse problems and conclude whether calcite dissolution/precipitation is relevant or not. This stepwise strategy allows us to identify the relevance of a given chemical process by solving the inverse problem under alternative scenarios in which the process is either occurring or not.

With our best regards,

Rabia Slimani

Geochemical inverse modeling of chemical and isotopic data from groundwaters in Sahara (Ouargla basin, Algeria)

R. Slimani^a, A. Guendouz^b, F. Trolard^c, A.S. Moulla^d, B. Hamdi-Aïssa^a, G. Bourrié^c

^aUniv Ouargla, Fac. des sciences de la nature et de la vie, Lab. Biochimie des milieux désertiques, Ouargla 30000, Algeria

^bBlida University, Science and Engineering Faculty, P.O.Box 270 Soumaa, Blida, Algeria

^cINRA, UMR 1114 Emmah, Avignon, France

^dNuclear Research Centre, 16000 Algiers, Algeria

Abstract

New samples were collected in the three major Saharan aquifers namely, the “Continental Intercalaire” (CI), the “Complexe Terminal” (CT) and the Phreatic aquifer (Phr) and completed with unpublished more ancient chemical and isotopic data. Instead of classical Debye-Hückel extended law, Specific Interaction Theory (SIT) model, recently incorporated in Phreeqc 3.0 was used. Inverse modeling of hydrochemical data constrained by isotopic data was used here to quantitatively assess the influence of geochemical processes: at depth, the dissolution of salts from the geological formations during upward leakage *without evaporation* explains the transitions from CI to CT and to a first pole of Phr (pole I); near the surface, the dissolution of salts from sebkhas by rainwater explains another pole of Phr (pole II). In every case, secondary precipitation of calcite occurs during dissolution. All Phr waters result from the mixing of these two poles together with calcite precipitation and ion exchange processes. These processes are quantitatively assessed by Phreeqc model. Globally, gypsum dissolution and calcite precipitation were found to act as a carbon sink.

Keywords: hydrochemistry, stable isotopes, Sahara, Algeria

1. INTRODUCTION

A scientific study published in 2008 showed that 85% of the world population lives in the driest half of the Earth. More than 1 billion people residing in arid and semi-arid areas of the world have only access to little or no renewable water resources (OECD, 2008). In many arid regions such as Sahara, groundwater is the only source of water supply for domestic, agricultural or industrial purposes, causing most of the time overuse and / or degradation of water quality.

The groundwater resources of Ouargla basin (Lower-Sahara, Algerian) (Fig. 1) are contained in three main reservoirs (UNESCO, 1972; Eckstein and Eckstein, 2003; OSS, 2003, 2008):

- at the top, the phreatic aquifer (Phr), located in sandy gypsum permeable formations of Quaternary, is almost unexploited (only north of Ouargla) due to its salinity (50 g/L);

Email address: s1m_rabia@yahoo.fr (R. Slimani)

- 34 • in the middle, the “Complexe Terminal” (CT) aquifer, (Cornet and Gouscov, 1952; UN-
35 ESCO, 1972) which is the most exploited, and includes several aquifers in different geo-
36 logical formations. It circulates in one or two lithostratigraphic formations of the Eocene
37 and Senonian carbonates or Miopliocene sands;
- 38 • at the bottom, the “Continental Intercalaire” (CI) aquifer, where water is contained in the
39 lower Cretaceous continental formations (Barremian and Albian), mainly composed of
40 sandstones, sands and clays. It is only partially exploited because of its significant depth.

41 After use, waters are discharged in a closed system (endorheic basin) and constitute a poten-
42 tial hazard to the environment, to public health and may jeopardize the sustainability of agricul-
43 ture (rising of the phreatic aquifer watertable, extension of soil salinization and so on) (Hamdi-
44 Aïssa et al., 2004; Slimani, 2006). Several previous studies (Guendouz, 1985; Fontes et al., 1986;
45 Guendouz and Moulla, 1996; Edmunds et al., 2003; Guendouz et al., 2003; Hamdi-Aïssa et al.,
46 2004; Foster et al., 2006; OSS, 2008; Al-Gamal, 2011) tried, starting from chemical and isotopic
47 information (^2H , ^{18}O , ^{234}U , ^{238}U , ^{36}Cl) to best characterize the relationships between aquifers.
48 They were more specifically tackling the issue of the Continental Intercalaire recharge. These
49 investigations dealt particularly with water chemical facies, mapped isocontents of various pa-
50 rameters, and reported typical geochemical ratios ($[\text{SO}_4^{2-}]/[\text{Cl}^-]$, $[\text{Mg}^{2+}]/[\text{Ca}^{2+}]$) as well as other
51 correlations. Minerals / solutions equilibria were checked by computing saturation indices with
52 respect to calcite, gypsum, anhydrite and halite, but processes were only qualitatively assessed.

53 In the present study, new data were collected in order to characterize the hydrochemical and
54 the isotopic composition of the major aquifers in Ouargla’s region. They also aimed at identify-
55 ing the origin of the mineralization and water-rock interactions that occur along the flow. New
56 possibilities offered by progress in geochemical simulations were used. More specifically, the
57 inverse modeling of chemical reactions allows us to select the best conceptual model for the in-
58 terpretation of the geochemical evolution of the Ouargla aquifer. The stepwise inversion strategy
59 involves designing a list of the scenarios that includes the most plausible combinations of geo-
60 chemical processes, solving scenarios in a stepwise manner, and selecting the scenario that pro-
61 vides the best conceptual geochemical model (Dai et al., 2006). Inverse modeling with Phreeqc
62 3.0 was used to quantitatively assess the influence of the processes that explain the acquisition
63 of solutes for the different aquifers: dissolution, precipitation, mixing and ion exchange. This
64 results in constraints on mass balances as well as on the exchange of matter between aquifers.

65 2. METHODOLOGY

66 2.1. Presentation of the study area

67 The study area is located in the northeastern desert of Algeria “Lower-Sahara” (Le Houérou,
68 2009) near the city of Ouargla (Fig. 1), $31^\circ 54'$ to $32^\circ 1'$ N and $5^\circ 15'$ to $5^\circ 27'$ E, with a mean eleva-
69 tion of 134 (masl). It is located in the quaternary fossil valley of Oued Mya basin. Present climate
70 belongs to the arid Mediterranean-type (Dubief, 1963; Le Houérou, 2009; ONM, 1975/2013).
71 This climate is characterized by a mean annual temperature of 22.5°C , a yearly rainfall of
72 43.6 mm/yr and a very high evaporation rate of $2,138\text{ mm/yr}$.

73
74 Ouargla’s region and the entire Lower Sahara has experienced during its long geological
75 history alternating marine and continental sedimentation phases. During Secondary era, vertical

76 movements affected the Precambrian basement and Primary causing particularly progressive col-
77 lapse of its central part, along an axis passing substantially through the Oued Righ valley and the
78 upper portion of the valley oued Mya. According to (Furon, 1960), a epicontinental sea spread
79 to the Lower Eocene of northern Sahara. After the Oligocene, the sea gradually withdrew. It is
80 estimated at present that this sea did not reach Ouargla and transgression stopped at the edge of
81 the bowl (Lelièvre, 1969). The basin is carved into Miopliocene (MP) deposits, which alternate
82 with red sands, clays and sometimes marls; gypsum is not abundant and dated from Pontian (MP)
83 (Cornet and Gouscov, 1952; Dubief, 1953; Ould Baba Sy and Besbes, 2006). The continental
84 Pliocene consists of a local limestone crust with puddingstone or lacustrine limestone (Fig. 2),
85 shaped by eolian erosion into flat areas (regs). The Quaternary formations are lithologically com-
86 posed of alternating layers of permeable sand and relatively impermeable marl (Aumassip et al.,
87 1972; Chellat et al., 2014).

88 The exploitation of Miopliocene aquifer is ancient and at the origin of the creation of the
89 oasis (Lelièvre, 1969; Moulias, 1927). The piezometric level was higher (145 m a.s.l.) but over-
90 exploitation at the end of the XIXth century led to a catastrophic decrease of the resource, with
91 presently more than 900 boreholes (ANRH, 2011).

92 The exploitation of Senonian aquifer dates back to 1953 at a depth 140 m to 200 m depth,
93 with a small initial rate *ca.* 540 L mn⁻¹; two boreholes have been exploited since 1965 and 1969,
94 with a total flowrate *ca.* 2,500 L mn⁻¹, for drinking water and irrigation.

95 The exploitation of Albian aquifer dates back to 1956, with a piezometric level 405 m and a
96 pressure 22 kg cm⁻². Presently, two boreholes are exploited:

- 97 • El Hedeb I, 1,335 m depth, with a flowrate 141 L s⁻¹;
- 98 • El Hedeb II, 1,400 m depth, with a flowrate 68 L s⁻¹.

99 2.2. *Sampling and analytical methods*

100 The sampling scheme complies with the flow directions of the two formations (Phr and CT
101 aquifers); for the CI aquifer only five points are available, so it is impossible to choose a transect
102 (Fig. 3). Groundwater samples ($n = 107$) were collected during a field campaign in 2013, along
103 the main flow line of Oued Mya, 67 piezometers tap the phreatic aquifer, 32 wells tap the CT
104 aquifer and 8 boreholes tap the CI aquifer (Fig. 3). Analyses of Na⁺, K⁺, Ca²⁺, Mg²⁺, Cl⁻,
105 SO₄²⁻ and HCO₃⁻ were performed by ion chromatography at Algiers Nuclear Research Center
106 (CRNA). Previous and yet unpublished data (Guendouz and Moulla, 1996) sampled in 1996 are
107 used here too: 59 samples for Phr aquifer, 15 samples for CT aquifer and 3 samples for the CI
108 aquifer for chemical analyses, data ¹⁸O and ³H (Guendouz and Moulla, 1996).

109 2.3. *Geochemical method*

110 Phreeqc (Parkhurst and Appelo, 2013) was used to check minerals / solution equilibria us-
111 ing the specific interaction theory (SIT), *i.e.* the extension of Debye-Hückel law by Scatchard
112 and Guggenheim incorporated recently in Phreeqc 3.0. Inverse modeling was used to calculate
113 the number of minerals and gases' moles that must respectively dissolve or precipitate/degas to
114 account for the difference in composition between initial and final water end members (Plum-
115 mer and Back, 1980; Kenoyer and Bowser, 1992; Deutsch, 1997; Plummer and Sprinkle, 2001;
116 Güler and Thyne, 2004; Parkhurst and Appelo, 2013). This mass balance technique has been
117 used to quantify reactions controlling water chemistry along flow paths (Thomas et al., 1989).

118 It is also used to quantify the mixing proportions of end-member components in a flow system
119 (Kuells et al., 2000; Belkhiri et al., 2010, 2012).

120 The Inverse modeling involves designing a list of the scenarios that includes the most plau-
121 sible combinations of geochemical processes. For example, the way to identify whether calcite
122 dissolution/precipitation is relevant or not consists of solving the inverse problem under two
123 alternate scenarios: (1) considering a geochemical system in which calcite is present, and (2)
124 considering a geochemical system without calcite. After solving the two scenarios, it is usually
125 possible to select the better result as the solution of the inverse problems and conclude whether
126 calcite dissolution/precipitation is relevant or not. This stepwise strategy allows us to identify the
127 relevance of a given chemical process by solving the inverse problem under alternative scenarios
128 in which the process is either occurring or not.

129 3. RESULTS AND DISCUSSION

130 Tables 1 to 5 illustrate the results of the chemical and the isotopic analyses. Samples are
131 ordered according to an increasing salt content that was estimated from their specific electric
132 conductivity (EC). In both phreatic and CT aquifers, temperature is close to 25 °C, while for
133 CI aquifer, temperature is close to 50 °C. The results presented in those tables are raw ana-
134 lytical data that were corrected for defects of charge balance before computing activities with
135 Phreeqc. As analytical errors could not be ascribed to a specific analyte, the correction was
136 made proportionally. The corrections do not affect the anions to anions mole ratios such as for
137 $[\text{HCO}_3^-]/([\text{Cl}^-] + 2[\text{SO}_4^{2-}])$ or $[\text{SO}_4^{2-}]/[\text{Cl}^-]$, whereas they affect the cation to anion ratio such
138 as for $[\text{Na}^+]/[\text{Cl}^-]$.

139 3.1. Characterization of chemical facies of the groundwater

140 Piper diagrams drawn for the studied groundwaters (Fig. 4) broadly show a scatter plot
141 dominated by a Chloride-Sodium facies. However, when going into small details, the widespread
142 chemical facies of the Phr aquifer is closer to the NaCl pole than those of CI and CT aquifers. The
143 facies of the Phreatic aquifer most concentrated samples are in the following order: Ca-sulfate <
144 Na-sulfate = Mg-sulfate < Na-chloride. This sequential order of solutes is comparable to that of
145 other groundwater occurring in North Africa, and especially in the neighboring area of the chotts
146 (depressions where salts concentrate by evaporation) Merouane and Melrhir (Vallès et al., 1997;
147 Hamdi-Aïssa et al., 2004).

148 3.2. Spatial distribution of the mineralization

149 The salinity of the phreatic aquifer varies considerably depending on the location (near wells
150 or drains) and time (influence of irrigation) (Fig. 5a).

151 Its salinity is low around irrigated and fairly well-drained areas, such as the palm groves of
152 Hassi Miloud, just north of Ouargla (Fig. 3) that benefit from freshwater and are drained to the
153 sebkha Oum el Raneb. However, the three lowest salinity values are observed in the wells of
154 Ouargla palm-grove itself, where the Phr aquifer watertable is deeper than 2 m.

155 Conversely, the highest salinity waters are found in wells drilled in the chotts and sebkhas (a
156 sebkha is the central part of a chott where salinity is the largest) (Safioune and Oum er Raneb)
157 where the aquifer is often shallower than 50 cm.

158 The salinity of the Complexe Terminal (Miopliocene) aquifer (Fig. 5b) is much lower than
159 that of the Phr aquifer, and ranges from 1 to 2 g/L; however, its hardness is larger and it contains

160 more sulfate, chloride and sodium than the waters of the Senonian formations and those of the
161 CI aquifer. The salinity of the Senonian aquifer ranges from 1.1 to 1.7 g/L , while the average
162 salinity of the Continental Intercalaire is 0.7 g/L (Fig. 5c).

163 A likely contamination of the Miopliocene aquifer by phreatic groundwaters through casing
164 leakage in an area where water is heavily loaded with salt and therefore particularly aggressive
165 cannot be excluded.

166 3.3. Saturation Indices

167 The calculated saturation indices reveal that waters from CI at 50 °C are close to equilibrium
168 with respect to calcite, except for 3 samples that are slightly oversaturated. They are however all
169 undersaturated with respect to gypsum (Fig. 6).

170 Moreover, they are oversaturated with respect to dolomite and undersaturated with respect to
171 anhydrite and halite (Fig. 7).

172 Waters from CT and phreatic aquifers show the same pattern, but some of them are more
173 largely oversaturated with respect to calcite, at 25 °C.

174 However, several phreatic waters (P031, P566, PLX4, PL18, P002, P023, P116, P066, P162
175 and P036) that are located in the sebkhas of Sefioune, Oum-er-Raneb, Bamendil and Ain el
176 Beida's chott are saturated with gypsum and anhydrite. This is in accordance with high evapora-
177 tive environments found elsewhere (UNESCO, 1972; Hamdi-Aïssa et al., 2004; Slimani, 2006).

178 No significant saturation indices' evolution from the south to the north upstream and down-
179 stream of Oued Mya (Fig. 7) is observed. This suggests that the acquisition of mineralization
180 is due to geochemical processes that have already reached equilibrium or steady state in the
181 upstream areas of Ouargla.

182 3.4. Change of facies from the carbonated pole to the evaporites' pole

183 The facies shifts progressively from the carbonated (CI and CT aquifers) to the evaporites'
184 one (Phr aquifer) with an increase in sulfates and chlorides at the expense of carbonates (SI
185 of gypsum, anhydrite and halite). This is illustrated by a decrease of the following two ratios:
186 $[HCO_3^-]/([Cl^-] + 2[SO_4^{2-}])$ (Fig. 8) from 0.2 to 0 and of the ratio $[SO_4^{2-}]/[Cl^-]$ from 0.8 to
187 values ranging from 0.3 and 0 (Fig. 9) while salinity increases. Carbonate concentrations tend
188 towards very small values, while it is not the case for sulfates. This is due to both gypsum
189 dissolution and calcite precipitation.

190 Chlorides in groundwater may come from three different sources: (i) ancient sea water en-
191 trapped in sediments; (ii) dissolution of halite and related minerals that are present in evaporite
192 deposits and (iii) dissolution of dry fallout from the atmosphere, particularly in these arid regions
193 (Matiatos et al., 2014; Hadj-Ammar et al., 2014).

194 For most of the sampled points the $[Na^+]/[Cl^-]$ ratio remains close to 1, but significant ranges
195 are observed: from 0.85 to 1.26 for CI aquifer, from 0.40 to 1.02 for the CT aquifer and from 0.13
196 to 2.15 for the Phr aquifer. All the measured points from the three considered aquifers are more
197 or less linearly scattered around the unity slope straight line that stands for halite dissolution
198 (Fig. 10). The latter appears as the most dominant reaction occurring in the medium. However,
199 at very high salinity, Na^+ seems to swerve from the straight line, towards smaller values.

200 A further scrutiny of (Fig. 10) shows that CI waters are very close to the 1:1 line. CT
201 waters are enriched in both Na^+ and Cl^- but slightly lower than the 1:1 line while phreatic waters
202 are largely enriched and much more scattered. CT waters are closer to the seawater mole ratio
203 (0.858), but some lower values imply a contribution from another source of chloride than halite

204 or from entrapped seawater. Conversely, a $[\text{Na}^+]/[\text{Cl}^-]$ ratio larger than 1 is observed for phreatic
205 waters, which implies the contribution of another source of sodium, most likely sodium sulfate,
206 that is present as mirabilite or thenardite in the chotts and the sebkhas areas.

207 $[\text{Br}^-]/[\text{Cl}^-]$ ratio ranges from 2×10^{-3} to 3×10^{-3} . The value of this molar ratio for halite is
208 around 2.5×10^{-3} , which matches the aforementioned range and confirms that halite dissolution
209 is the most dominant reaction taking place in the studied medium.

210 In these aquifers, calcium originates both from carbonate and sulfate (Fig. 11 and 12). Three
211 samples from CI aquifer are close to the $[\text{Ca}^{2+}]/[\text{HCO}_3^-]$ 1:2 line, while calcium sulfate disso-
212 lution explains the excess of calcium. However, a small but significant number of samples (9)
213 from phreatic aquifer are depleted in calcium, and plot under the $[\text{Ca}^{2+}]/[\text{HCO}_3^-]$ 1:2 line. This
214 cannot be explained by precipitation of calcite, as some are undersaturated with respect to that
215 mineral, while others are oversaturated.

216 In this case, a cation exchange process seems to occur leading to a preferential adsorption
217 of divalent cations, with a release of Na^+ . This is confirmed by the inverse modeling that is
218 developed below and which implies Mg^{2+} fixation and Na^+ and K^+ releases.

219 Larger sulfate values observed in the phreatic aquifer (Fig. 12) with $[\text{Ca}^{2+}]/[\text{SO}_4^{2-}] < 1$ can
220 be attributed to a sodium-magnesium sulfate dissolution from a mineral bearing such elements.
221 This is for instance the case of bloedite.

223 3.5. Isotope geochemistry

224 CT and CI aquifer exhibit depleted and homogeneous ^{18}O contents, ranging from -8.32‰
225 to -7.85‰ . This was already previously reported by many authors (Edmunds et al., 2003;
226 Guendouz et al., 2003; Moulla et al., 2012). On the other hand, ^{18}O values for the phreatic
227 aquifer are widely dispersed and vary between -8.84‰ to 3.42‰ (Table 6).

228 Waters located north of the Hassi Miloud to Sebkheth Safioune axis are more enriched in
229 heavy isotopes and therefore more evaporated. In that area, water table is close to the surface
230 and mixing of both CI and CT groundwaters with phreatic ones through irrigation is nonexistent.
231 Conversely, waters located south of Hassi Miloud up to Ouargla city show depleted values. This
232 is the clear fingerprint of a contribution to the Phr waters from the underlying CI and CT aquifers
233 (Gonfiantini et al., 1975; Guendouz, 1985; Fontes et al., 1986; Guendouz and Moulla, 1996).

234 Phreatic waters result from a mixing of two end-members. An evidence for this is given
235 by considering the ($[\text{Cl}^-]$, ^{18}O) relationship (Fig. 13). The two poles are: i) a first pole of ^{18}O
236 depleted groundwater (Fig. 14), and ii) another pole of ^{18}O enriched groundwater with positive
237 values and a high salinity. The latter is composed of phreatic waters occurring in the northern
238 part of the study region.

239 Pole I represents the waters from CI and CT whose isotopic composition is depleted in ^{18}O
240 (average value around -8.2‰) (Fig. 13). They correspond to an old water recharge (palæorecharge);
241 whose age estimated by means of ^{14}C , exceeds 15.000 years BP (Guendouz, 1985; Guendouz and
242 Michelot, 2006). So, it is not a water body that is recharged by recent precipitation. It consists of
243 CI and CT groundwaters and partly of phreatic waters, and can be ascribed to an upward leakage
244 favored by the extension of faults near Amguid El-Biod dorsal.

245 Pole II, observed in Sebkheth Safioune, can be ascribed to the direct dissolution of surficial
246 evaporitic deposits conveyed by evaporated rainwater.

247 Evaporation alone cannot explain the distribution of data that is observed (Fig. 13). An
248 evidence for this is given in a semi-logarithmic plot (Fig. 14), as classically obtained according
249 to the simple approximation of Rayleigh equation (cf. Appendix):

$$\delta^{18}\text{O} \approx 1000 \times (1 - \alpha) \log[\text{Cl}^-] + cte, \quad (1)$$

$$\approx -\epsilon \log[\text{Cl}^-] + cte, \quad (2)$$

250 where α is the fractionation factor during evaporation, and $\epsilon \equiv -1000 \times (1 - \alpha)$ is the enrich-
 251 ment factor (Ma et al., 2010; Chkir et al., 2009).

252 CI and CT waters are better separated in the semi-logarithmic plot because they are differen-
 253 tiated by their chloride content. According to equation (1), simple evaporation gives a straight
 254 line (solid line in Fig. 14). The value of ϵ used is the value at 25 °C, which is equal to -73.5 .
 255 There is only one sample (P115) on the evaporation straight line, which could be considered as
 256 an outlier in Fig. 13 ($[\text{Cl}^-] \approx 0$). All other samples fit on the logarithmic curve derived from the
 257 mixing line illustrated by Fig. 13.

258 The phreatic waters that are close to pole I (Fig. 13) correspond to groundwaters occurring in
 259 the edges of the basin (Hassi Miloud, piezometer P433) (Fig. 14). They are low-mineralized and
 260 acquire their salinity via two processes namely: dissolution of evaporites along their underground
 261 transit up to Sebket Safioune and dilution through upward leakage by the less-mineralized wa-
 262 ters of CI and CT aquifers (for example Hedeb I for CI and D7F4 for CT) (Fig. 14) (Guendouz,
 263 1985; Guendouz and Moulla, 1996).

264 The rates of the mixing that are due to upward leakage from CI to CT towards the phreatic
 265 aquifer can be calculated by means of a mass balance equation. It only requires knowing the δ
 266 values of each fraction that is involved in the mixing process.

267 The δ value of the mixture is given by:

$$\delta_{\text{mix}} = f_1 \times \delta_1 + f_2 \times \delta_2 \quad (3)$$

268 where f_1 is the fraction of CI aquifer, f_2 the fraction of the CT and δ_1 , δ_2 are the respective
 269 isotope contents.

270 Average values of mixing fractions from each aquifer to the phreatic waters computed by
 271 means of equation (3) gave the rates of 65 % for CI aquifer and 35% for CT aquifer.

272 A mixture of a phreatic water component that is close to pole I (*i.e.* P433) with another one
 273 which is rather close to pole II (*i.e.* P039) (Fig. 13 and 14), for an intermediate water with a $\delta^{18}\text{O}$
 274 signature ranging from -5‰ to -2‰ gives mixture fraction values of 52 % for pole I and 48 %
 275 for pole II. Isotope results will be used to independently cross-check the validity of the mixing
 276 fractions derived from an inverse modeling involving chemical data (*cf. infra*).

277 Turonian evaporites are found to lie in between CI deep aquifer, and the Senonian and
 278 Miocene formations bearing CT aquifer. CT waters can thus simply originate from ascend-
 279 ing CI waters that dissolve Turonian evaporites, a process which does involve any change in ^{18}O
 280 content. Conversely, phreatic waters result to a minor degree from evaporation, and mostly from
 281 dissolution of sebkhas evaporites by ^{18}O enriched rainwater and mixing with CI-CT waters.

282 3.5.1. Tritium content of water

283 Tritium contents of Phr aquifer are relatively small (Table 6), they vary between 0 and 8 TU.
 284 Piezometers PZ12, P036 and P068 show values close to 8 TU, piezometers P018, P019, P416,
 285 P034, P042 and P093 exhibit values ranging between 5 and 6 TU, and the rest of the samples'
 286 concentrations are lower than 2 TU.

287 This values are dated back to November 1992 so they are old values. This is the main reason
 288 why they are considered high comparatively to what is expected to be found nowadays. In fact,

289 at present times, tritium figures have fallen lower than 5 TU in precipitation measured in the
290 northern part of the country.

291 The comparison of these results with that of precipitation which was 16 TU in 1992 was
292 collected from the National Agency for Water Resources station from Ouargla).

293 This value seems to be high but we can note that we are in an arid area (desert) where precip-
294 itation is very scarce and irregular. Precipitation takes place in the form of sudden thunderstorms
295 in an unsaturated atmosphere and a great part of this precipitation evaporates back into the mois-
296 ture unsaturated atmosphere sometimes during many cycles. Consequently, an enrichment in
297 tritium happens because when water evaporates back, the lightest fractions (isotopes) are the
298 ones that evaporate first causing an enrichment in Tritium in the remaining fraction. The 16 TU
299 value would thus correspond then to a rainy event that had happened during the same sampling
300 period (Nov. 1992). It's the only available value and it is not a weighted mean for a long period
301 of time. It is the most representative value for that region and for that time. Unfortunately, all the
302 other stations (Algiers, Ankara, and Tenerife) (Martinelli et al., 2014) are subject to a completely
303 different climatic regime and besides the fact that they have more recent values, can absolutely
304 not be used for our case. Therefore all the assumptions based on recent tritium rain values do not
305 apply to this study.

306 Depleted contents in ^{18}O and low tritium concentrations for phreatic waters fit well the mix-
307 ing scheme and confirm the contribution from the older and deeper CI/CT groundwaters. The
308 affected areas were clearly identified in the field and correspond to locations that are subject to
309 a recycling and a return of irrigation waters whose origin are CI/CT boreholes. Moreover, the
310 mixing that is clearly brought to light by the Cl^- vs. ^{18}O diagrams (Fig. 13 and 14) could partly
311 derive from an ascending drainage from the deep and confined CI aquifer (exhibiting depleted ho-
312 mogenous ^{18}O contents and very low tritium), a vertical leakage that is favoured by the Amguid
313 El-biod highly faulted area (Guendouz and Moulla, 1996; Edmunds et al., 2003; Guendouz et al.,
314 2003; Moulla et al., 2012).

315 3.6. Inverse modeling

316 We assume that the relationship between ^{18}O and Cl^- data obtained in 1996 is stable with
317 time, which is a logical assumption as times of transfer from CI to both CT and Phr are very long.
318 Considering both ^{18}O and Cl^- data, CI, CT and Phr data populations can be categorized. The CI
319 and CT do not show appreciable ^{18}O variations, and can be considered as a single population.
320 The Phr samples consist however of different populations: Pole I, with $\delta^{18}\text{O}$ values close to -8,
321 and small Cl^- concentrations, more specifically less than 35 mmol L^{-1} ; Pole II, with $\delta^{18}\text{O}$ values
322 larger than 3, and very large Cl^- concentrations, more specifically larger than $4,000 \text{ mmol L}^{-1}$
323 (Table 7); intermediate Phr samples result from mixing between poles I and II (mixing line in
324 Fig. 13, mixing curve in Fig. 14) and from evaporation of pole I (evaporation line in Fig. 14).

325 The mass-balance modeling has shown that relatively few phases are required to derive ob-
326 served changes in water chemistry and to account for the hydrochemical evolution in Ouargla's
327 region. The mineral phases' selection is based upon geological descriptions and analysis of rocks
328 and sediments from the area (OSS, 2003; Hamdi-Aïssa et al., 2004).

329 The inverse model was constrained so that mineral phases from evaporites including gypsum,
330 halite, mirabilite, glauberite, sylvite and bloedite were set to dissolve until they reach saturation,
331 and calcite, dolomite were set to precipitate once they reached saturation. Cation exchange reac-
332 tions of Ca^{2+} , Mg^{2+} , K^+ and Na^+ on exchange sites were included in the model to check which
333 cations are adsorbed or desorbed during the process. Dissolution and desorption contribute as

334 positive terms in the mass balance, as elements are released in solution. On the other hand,
335 precipitation and adsorption contribute as negative terms, while elements removed from the so-
336 lution. $\text{CO}_{2(g)}$ dissolution is considered by Phreeqc as a dissolution of a mineral, whereas $\text{CO}_{2(g)}$
337 degassing is dealt with as if it were a mineral precipitation.

338 Inverse modelling leads to a quantitative assessment of the different solutes' acquisition pro-
339 cesses and a mass balance for the salts that are dissolved or precipitated from CI, CT and Phr
340 groundwaters (Fig. 14, Table 8), as follows:

- 341 • transition from CI to CT involves gypsum, halite and sylvite dissolution, and some ion
342 exchange namely calcium and potassium fixation on exchange sites against magnesium
343 release, with a very small and quite negligible amount of $\text{CO}_{2(g)}$ degassing. The maximum
344 elemental concentration fractional error equals 1%. The model consists of a minimum
345 number of phases (*i.e.* 6 solid phases and $\text{CO}_{2(g)}$); Another model implies as well dolomite
346 precipitation with the same fractional error;
- 347 • transition from CT to an average water component of pole I involves dissolution of halite,
348 sylvite, and bloedite from Turonian evaporites, with a very tiny calcite precipitation. The
349 maximum fractional error in elemental concentration is 4%. Another model implies $\text{CO}_{2(g)}$
350 escape from the solution, with the same fractional error. Large amounts of Mg^{2+} and SO_4^{2-}
351 are released within the solution (Sharif et al., 2008; Li et al., 2010; Carucci et al., 2012);
- 352 • the formation of Phr pole II can be modeled as being a direct dissolution of salts from the
353 sebkha by rainwater with positive $\delta^{18}\text{O}$; the most concentrated water (P036 from Sebkhet
354 Safioune) is taken here for pole II, and pure water as rainwater. In a decreasing order
355 of amounts respectively involved in that process, halite, sylvite, gypsum and huntite dis-
356 solve, and little calcite precipitates while some Mg^{2+} are released versus K^+ fixation on
357 exchange sites. The maximum elemental fractional error in the concentration is equal to
358 0.004%. Another model implies dolomite precipitation with some more huntite dissolv-
359 ing, instead of calcite precipitation, but salt dissolution and ion exchange are the same.
360 Huntite, dolomite and calcite stoichiometries are linearly related, so both models can fit
361 field data, but calcite precipitation is preferred compared to dolomite precipitation at low
362 temperature;
- 363 • the origin of all phreatic waters can be explained by a mixing in variable proportions of
364 pole I and pole II. For instance, waters from pole I and pole II can easily be separated by
365 their $\delta^{18}\text{O}$ respectively close to -8‰ and 3.5‰ (Fig. 13 and 14). Mixing the two poles
366 is of course not an inert reaction, but rather results in the dissolution and the precipitation
367 of minerals. Inverse modeling is then used to compute both mixing rates and the extent
368 of matter exchange between soil and solution. For example, a phreatic water (piezometer
369 P068) with intermediate values ($\delta^{18}\text{O} = -3$ and $[\text{Cl}^-] \approx 2\text{ M}$) is explained by the mixing
370 of 58% water from pole I and 42% from pole II. In addition, calcite precipitates, Mg^{2+}
371 fixes on exchange sites, against Na^+ and K^+ , gypsum dissolves as well as a minor amount
372 of huntite (Table 8). The maximum elemental concentration fractional error is 2.5% and
373 the mixing fractions' weighted the $\delta^{18}\text{O}$ is -3.17‰ , which is very close to the measured
374 value (-3.04‰). All the other models, making use of a minimum number of phases, and
375 not taking into consideration ion exchange reactions are not found compatible with isotope
376 data. Mixing rates obtained with such models are for example 98% of pole I and 0.9% of

377 pole II, which leads to a $\delta^{18}O = (-7.80\text{‰})$ which is quite far for the real measured value
378 (-3.04‰) .

379 The main types of groundwaters occurring in Ouargla basin are thus explained and could
380 quantitatively be reconstructed. An exception is however sample P115, which is located exactly
381 on the evaporation line of Phr pole I. Despite numerous attempts, it could not be quantitatively
382 rebuilt. Its 3H value (6.8) indicates that it is derived from a more or less recent water component
383 with very small salt content, most possibly affected by rainwater and some preferential flow
384 within the piezometer. As this is the only sample on this evaporation line, there remains a doubt
385 on its significance.

386 Globally, the summary of mass transfer reactions occurring in the studied system (Table 8)
387 shows that gypsum dissolution results in calcite precipitation and $CO_{2(g)}$ dissolution, thus acting
388 as an inorganic carbon sink.

389 4. CONCLUSIONS

390 Groundwater hydrochemistry is a good record indicator for the water-rock interactions that
391 occur along the groundwater flowpath. The mineral load reflects well the complex processes
392 taking place while water circulates underground since its point of infiltration.

393 The hydrochemical study of the aquifer system occurring in Ouargla's basin allowed us to
394 identify the origin of its mineralization. Waters exhibit two different facies: sodium chloride and
395 sodium sulfate for the phreatic aquifer (Phr), sodium sulfate for the Complexe Terminal (CT)
396 aquifer and sodium chloride for the Continental Intercalaire (CI) aquifer. Calcium carbonate pre-
397 cipitation and evaporite dissolution explain the facies change from carbonate to sodium chloride
398 or sodium sulfate. However reactions imply many minerals with common ions, deep reactions
399 without evaporation as well as shallow processes affected by both evaporation and mixing. Those
400 processes are separated by considering both chemical and isotopic data, and quantitatively ex-
401 plained making use of an inverse geochemical modeling. The main result is that Phr waters do
402 not originate simply from infiltration of rainwater and dissolution of salts from the sebkhas. Con-
403 versely, Phr waters are largely influenced by the upwardly mobile deep CT and CI groundwaters,
404 fractions of the latter interacting with evaporites from Turonian formations. Phreatic waters oc-
405 currence is explained as a mixing of two end-member components: pole I, which is very close to
406 CI and CT, and pole II, which is highly mineralized and results from the dissolution by rainwater
407 of salts from the sebkhas.

408 At depth, CI leaks upwardly and dissolves gypsum, halite and sylvite, with some ion ex-
409 change, to give waters of CT aquifer composition.

410 CT transformation into Phr pole I waters involves the dissolution of Turonian evaporites
411 (halite, sylvite and bloedite) with minor calcite precipitation.

412 At the surface, direct dissolution by rainwater of salts from sebkhas (halite, sylvite, gypsum
413 and some huntite) with precipitation of calcite and Mg^{2+}/K^+ ion exchange results in pole II Phr
414 composition.

415 All phreatic groundwaters result from a mixing of pole I and pole II water that is accompanied
416 by calcite precipitation, fixation of Mg^{2+} on ion exchange sites against the release of K^+ and Na^+ .

417 Moreover, some $CO_{2(g)}$ escapes from the solution at depth, but dissolves much more at the
418 surface. The most complex phenomena occur during the dissolution of Turonian evaporites while
419 CI leaks upwardly towards CT, and from Phr I to Phr II, while the transition from CT to Phr I

420 implies a very limited number of phases. Globally, gypsum dissolution and calcite precipitation
 421 processes both act as an inorganic carbon sink.

422 ACKNOWLEDGEMENTS

423 The authors wish to thank the staff members of the National Agency for Water Resources in
 424 Ouargla (ANRH) and the Laboratory of Algerian waters (ADE) for the support provided to the
 425 Technical Cooperation within which this work was carried out. Analyses of ^{18}O were funded by
 426 the project CDTN / DDHI (Guendouz and Moulla, 1996). The supports of University of Ouargla
 427 and of INRA for travel grants of R. Slimani and G. Bourrié are gratefully acknowledged too.

428 APPENDIX

429 According to a simple Rayleigh equation, the evolution of the heavy isotope ratio in the
 430 remaining liquid R_l is given by:

$$R_l \approx R_{l,0} \times f_l^{\alpha-1}, \quad (4)$$

431 where f_l is the fraction remaining liquid and α the fractionation factor.

432 The fraction remaining liquid is derived from chloride concentration, as chloride can be con-
 433 sidered as conservative during evaporation: all phreatic waters are undersaturated with respect to
 434 halite, that precipitates only in the last stage. Hence, the following equation holds:

$$f_l \equiv \frac{n_{w,1}}{n_{w,0}} = \frac{[\text{Cl}^-]_0}{[\text{Cl}^-]_1}. \quad (5)$$

435 By taking natural logarithms, one obtains:

$$\ln R_l \approx (1 - \alpha) \times \ln[\text{Cl}^-] + cte, \quad (6)$$

436 As, by definition,

$$R_l \equiv R_{std.} \times \left(1 + \frac{\delta^{18}\text{O}}{1000}\right), \quad (7)$$

437 one has:

$$\ln R_l \equiv \ln R_{std.} + \ln\left(1 + \frac{\delta^{18}\text{O}}{1000}\right), \quad (8)$$

$$\approx \ln R_{std.} + \frac{\delta^{18}\text{O}}{1000}, \quad (9)$$

438 hence, with base 10 logarithms:

$$\delta^{18}\text{O} \approx 1000(1 - \alpha) \log[\text{Cl}^-] + cte, \quad (10)$$

$$\approx -\epsilon \log[\text{Cl}^-] + cte, \quad (11)$$

439 where as classically defined $\epsilon = 100(\alpha - 1)$ is the enrichment factor.

440 **References**

- 441 Al-Gamal, S.A., 2011. An assessment of recharge possibility to North-Western Sahara Aquifer System (NWSAS) using
 442 environmental isotopes. *Journal of Hydrology* 398, 184 – 190.
- 443 ANRH, 2011. Inventaire des forages de la Wilaya de Ouargla. Rapport technique. Agence Nationale des Ressources
 444 Hydrauliques.
- 445 Aumassip, G., Dagorne, A., Estorges, P., Lefèvre-Witier, P., Mahrour, F., Nesson, C., Rouvillois-Brigol, M., Trecolle, G.,
 446 1972. Aperçus sur l'évolution du paysage quaternaire et le peuplement de la région de Ouargla. *Libyca*, 205–257.
- 447 Belkhir, L., Boudoukha, A., Mouni, L., Baouz, T., 2010. Application of multivariate statistical methods and inverse
 448 geochemical modeling for characterization of groundwater — A case study: Ain Azel plain (Algeria). *Geoderma*
 449 159, 390 – 398.
- 450 Belkhir, L., Mouni, L., Boudoukha, A., 2012. Geochemical evolution of groundwater in an alluvial aquifer: Case of El
 451 Eulma aquifer, East Algeria. *Journal of African Earth Sciences* 66–67, 46 – 55.
- 452 Carucci, V., Petitta, M., Aravena, R., 2012. Interaction between shallow and deep aquifers in the Tivoli Plain (Central
 453 Italy) enhanced by groundwater extraction: A multi-isotope approach and geochemical modeling. *Applied Geochem-*
 454 *istry* 27, 266 – 280. URL: <http://www.sciencedirect.com/science/article/pii/S0883292711004628>,
 455 doi:<http://dx.doi.org/10.1016/j.apgeochem.2011.11.007>.
- 456 Chellat, S., Bourefis, A., Hamdi-Aïss, a.B., Djerrab, A., 2014. Paléoenvironnemental reconstitution of Mio-pliocenes
 457 sandstones of the lower-Sahara at the base of exoscopic and sequential analysis. *Pensee Journal* 76, 34 – 51.
- 458 Chkir, N., Guendouz, A., Zouari, K., Hadj Ammar, F., Moulla, A., 2009. Uranium isotopes in groundwater from the
 459 continental intercalaire aquifer in Algerian Tunisian Sahara (Northern Africa). *Journal of Environmental Radioac-*
 460 *tivity* 100, 649 – 656. URL: <http://www.sciencedirect.com/science/article/pii/S0265931X09001143>,
 461 doi:<http://dx.doi.org/10.1016/j.jenvrad.2009.05.009>.
- 462 Cornet, A., Gouscov, N., 1952. Les eaux du Crétacé inférieur continental dans le Sahara algérien: nappe dite "Albien",
 463 in: *Congrès géologique international, Alger*. p. 30.
- 464 Dai, Z., Samper, J., Ritzi, R., 2006. Identifying geochemical processes by inverse modeling of multicomponent reactive
 465 transport in the aquia aquifer. *Geosphere* 2, 210–219.
- 466 Deutsch, W., 1997. *Groundwater Chemistry-Fundamentals and Applications to Contamination*. New York.
- 467 Dubief, J., 1953. *Essai sur l'hydrologie superficielle au Sahara*. Direction du service de la colonisation et de
 468 l'hydraulique, Service des études scientifiques.
- 469 Dubief, J., 1963. *Le climat du Sahara*. Hors-série, Institut de recherches sahariennes.
- 470 Eckstein, G., Eckstein, Y., 2003. A hydrogeological approach to transboundary ground water resources and international
 471 law. *American University International Law Review* 19, 201–258.
- 472 Edmunds, W., Guendouz, A., Mamou, A., Moulla, A., Shand, P., Zouari, K., 2003. Groundwater evolution in the
 473 continental intercalaire aquifer of southern Algeria and Tunisia: trace element and isotopic indicators. *Applied*
 474 *Geochemistry* 18, 805–822.
- 475 Fontes, J., Yousfi, M., Allison, G., 1986. Estimation of long-term, diffuse groundwater discharge in the northern sahara
 476 using stable isotope profiles in soil water. *Journal of Hydrology* 86, 315 – 327.
- 477 Foster, S., Margat, J., Droubi, A., 2006. Concept and importance of nonrenewable resources. Number 10 in IHP-VI
 478 *Series on Groundwater, UNESCO*.
- 479 Furon, R., 1960. *Géologie de l'Afrique*. 2eme édition, Payot.
- 480 Güler, C., Thyne, G., 2004. Hydrologic and geologic factors controlling surface and groundwater chemistry in Indian
 481 wells–Owens valley area, southeastern California, USA. *Journal of Hydrology* 285, 177–198.
- 482 Gonfiantini, R., Conrad, G., Fontes, J.C., Sauzay, G., Payne, B., 1975. Étude isotopique de la nappe du Continental
 483 Intercalaire et de ses relations avec les autres nappes du Sahara septentrional. *Isotope Techniques in Groundwater*
 484 *Hydrology* 1, 227–241.
- 485 Guendouz, A., 1985. Contribution à l'étude hydrochimique et isotopique des nappes profondes du Sahara nord-est
 486 septentrional, Algérie. Phd thesis. Université d'Orsay, France.
- 487 Guendouz, A., Michelot, J., 2006. Chlorine-36 dating of deep groundwater from northern Sahara. *Journal of Hydrology*
 488 328, 572–580.
- 489 Guendouz, A., Moulla, A., 1996. Étude hydrochimique et isotopique des eaux souterraines de la cuvette de Ouargla,
 490 Algérie. Rapport technique. CDTN/DDHI.
- 491 Guendouz, A., Moulla, A., Edmunds, W., Zouari, K., Shands, P., Mamou, A., 2003. Hydrogeochemical and isotopic
 492 evolution of water in the complex terminal aquifer in Algerian Sahara. *Hydrogeology Journal* 11, 483–495.
- 493 Hadj-Ammar, F., Chkir, N., Zouari, K., Hamelin, B., Deschamps, P., Aigoun, A., 2014. Hydro-
 494 geochemical processes in the Complexe Terminal aquifer of southern Tunisia: An integrated investi-
 495 gation based on geochemical and multivariate statistical methods. *Journal of African Earth Sciences*
 496 100, 81 – 95. URL: <http://www.sciencedirect.com/science/article/pii/S1464343X14001940>,
 497 doi:<http://dx.doi.org/10.1016/j.jafrearsci.2014.06.015>.

- 498 Hamdi-Aïssa, B., Vallès, V., Aventurier, A., Ribolzi, O., 2004. Soils and brines geochemistry and mineralogy of hyper
499 arid desert playa, Ouargla basin, Algerian Sahara. *Arid Land Research and Management* 18, 103–126.
- 500 Kenoyer, G., Bowser, C., 1992. Groundwater chemical evolution in a sandy aquifer in northern Wisconsin. *Water*
501 *Resources Research* 28, 591–600.
- 502 Kuells, C., Adar, E., Udluft, P., 2000. Resolving patterns of ground water flow by inverse hydrochemical modeling in a
503 semiarid Kalahari basin. *Tracers and Modelling in Hydrogeology* 262, 447–451.
- 504 Le Houérou, H., 2009. *Bioclimatology and biogeography of Africa*. Springer Verlag.
- 505 Lelièvre, R., 1969. Assainissement de la cuvette de Ouargla. rapports Géohydraulique n° 2. Ministère des Travaux
506 Publiques et de la construction.
- 507 Li, P., Qian, H., Wu, J., Ding, J., 2010. Geochemical modeling of groundwater in southern plain area of Pengyang
508 County, Ningxia, China. *Water Science and Engineering* 3, 282–291.
- 509 Ma, J., Pan, F., Chen, L., Edmunds, W., Ding, Z., Zhou, K., He, J., Zhou, K., Huang, T., 2010. Isotopic and geochemical
510 evidence of recharge sources and water quality in the Quaternary aquifer beneath Jinchang city, NW China. *Applied*
511 *Geochemistry* 25, 996–1007.
- 512 Martinelli, G., Chahoud, A., Dadomo, A., Fava, A., 2014. Isotopic features of emilia-romagna region
513 (north italy) groundwaters: Environmental and climatological implications. *Journal of Hydrology* 519, Part
514 B, 1928 – 1938. URL: <http://www.sciencedirect.com/science/article/pii/S0022169414007690>,
515 doi:<http://dx.doi.org/10.1016/j.jhydrol.2014.09.077>.
- 516 Matiatos, I., Alexopoulos, A., Godelitsas, A., 2014. Multivariate statistical analysis of the hydrogeochemical and isotopic
517 composition of the groundwater resources in northeastern Peloponnesus (Greece). *Science of The Total Environment*
518 476–477, 577 – 590. URL: <http://www.sciencedirect.com/science/article/pii/S0048969714000515>,
519 doi:<http://dx.doi.org/10.1016/j.scitotenv.2014.01.042>.
- 520 Moulias, D., 1927. L'eau dans les oasis sahariennes, organisation hydraulique, régime juridique. Phd thesis. Alger.
- 521 Moulla, A., Guendouz, A., Cherchali, M.H., Chaid, Z., Ouarezki, S., 2012. Updated geochemical and isotopic data
522 from the Continental Intercalaire aquifer in the Great Occidental Erg sub-basin (south-western Algeria). *Quaternary*
523 *International* 257, 64–73.
- 524 OECD, 2008. *OECD Environmental Outlook to 2030. Technical Report 1*. Organisation for Economic Cooperation and
525 Development.
- 526 ONM, 1975/2013. *Bulletins mensuels de relevé des paramètres climatologiques en Algérie*. Office national
527 météorologique.
- 528 OSS, 2003. *Système aquifère du Sahara septentrional*. Technical Report. Observatoire du Sahara et du Sahel.
- 529 OSS, 2008. *Système aquifère du Sahara septentrional (Algérie, Tunisie, Libye): gestion concertée d'un bassin trans-*
530 *frontalier*. Technical Report 1. Observatoire du Sahara et du Sahel.
- 531 Ould Baba Sy, M., Besbes, M., 2006. Holocene recharge and present recharge of the Saharan aquifers — a study by
532 numerical modeling, in: *International symposium - Management of major aquifers*.
- 533 Parkhurst, D., Appelo, C., 2013. *Description of Input and Examples for PHREEQC (Version 3) — A computer program*
534 *for speciation, batch-reaction, one-dimensional transport, and inverse geochemical calculations*. Technical Report 6.
535 U.S. Department of the Interior, U.S. Geological Survey. URL: <http://pubs.usgs.gov/tm/06/a43>.
- 536 Plummer, L., Back, M., 1980. The mass balance approach: application to interpreting the chemical evolution of hydro-
537 logical systems. *American Journal of Science* 280, 130–142.
- 538 Plummer, L., Sprinkle, C., 2001. Radiocarbon dating of dissolved inorganic carbon in groundwater from confined parts
539 of the upper Floridan aquifer, Florida, USA. *Journal of Hydrology* 9, 127–150.
- 540 Sharif, M., Davis, R., Steele, K., Kim, B., Kresse, T., Fazio, J., 2008. Inverse geochemical modeling of groundwater
541 evolution with emphasis on arsenic in the Mississippi River Valley alluvial aquifer, Arkansas (USA). *Journal of Hy-*
542 *drology* 350, 41 – 55. URL: <http://www.sciencedirect.com/science/article/pii/S0022169407007093>,
543 doi:<http://dx.doi.org/10.1016/j.jhydrol.2007.11.027>.
- 544 Slimani, R., 2006. Contribution à l'évaluation d'indicateurs de pollution environnementaux dans la région de Ouargla:
545 cas des eaux de rejets agricoles et urbaines. Master's thesis. Université de Ouargla.
- 546 Stumm, W., Morgan, J., 1999. *Aquatic Chemistry: Chemical Equilibria and Rates in Natural Waters*. John Wiley and
547 Sons.
- 548 Thomas, J., Welch, A., Preissler, A., 1989. Geochemical evolution of ground water in smith creek valley - a hydrologi-
549 cally closed basin in central Nevada, USA. *Applied Geochemistry* 4, 493–510.
- 550 UNESCO, 1972. *Projet ERESS, Étude des ressources en eau du Sahara septentrional*. Technical Report 10. UNESCO.
- 551 Vallès, V., Rezagui, M., Auque, L., Semadi, A., Roger, L., Zouggari, H., 1997. Geochemistry of saline soils in two arid
552 zones of the Mediterranean basin. I. Geochemistry of the Chott Melghir-Mehrouane watershed in Algeria. *Arid Soil*
553 *Research and Rehabilitation* 11, 71–84.

Table 1: Field and analytical data for the Continental Intercalaire aquifer.

Locality	Lat.	Long.	Elev.	Date	EC		T	pH	/mmolL ⁻¹									
					EC	EC			Alk	Cl ⁻	SO ₄ ²⁻	Na ⁺	K ⁺	Mg ²⁺	Ca ²⁺	Br ⁻		
Hebbs I	3,534,750	723,986	134.8	09/11/2012	2.01	46.5	7.65	3.5	5.8	6.79	10.7	0.63	2.49	3.3				
Hebbs I	3,534,750	723,986	134.8	1996	1.9	49.3	7.35	0.42	5.81	1.07	5.71	0.18	0.77	0.48	0.034			
Hebbs II	3,534,310	724,290	146.2	1996	2.02	47.4	7.64	0.58	6.19	1.22	5.06	0.2	1.28	0.82				
Aouinet Mousa	3,548,896	721,076	132.6	22/02/2013	2.2	48.9	7.55	1.28	6.49	1.28	5.65	0.16	1.14	1.17				
Aouinet Mousa	3,548,896	721,076	132.6	11/12/2010	2.2	48.9	7.55	3.19	9.8	3.89	6.3	0.69	5.71	1.27				
Hebbs I	3,534,750	723,986	134.8	22/02/2013	2.19	49.3	7.35	1.91	12.4	4.58	10.7	0.7	3.77	2.35				
Hebbs II	3,534,310	724,290	146.2	11/12/2010	2.26	47.4	7.64	2.11	13.1	5.24	13.9	0.53	4.53	1.41				
Hassi Khfif	3,591,659	721,636	110	24/02/2013	2.43	50.5	6.83	2.98	14.3	5.24	10.8	0.84	3.44	4.63	0.033			
Hassi Khfif	3,534,750	723,986	134.8	27/02/2013	2.01	46.5	7.65	3.46	15.1	7.67	11.8	0.51	5.57	5.16				
Hassi Khfif	3,591,659	721,636	110	09/11/2012	2	50.1	7.56	3.31	15.3	7.77	12.2	0.59	5.77	4.95				
El-Bour	3,560,264	720,366	160	22/02/2013	2.96	54.5	7.34	2.88	18.6	6.21	20.6	0.66	4.79	1.38				

Table 2: Field and analytical data for the Complex Terminal aquifer.

Locality	Site	Aquifer	Lat.	Long.	Elev.	Date	EC /mS cm ⁻¹	T /°C	pH	Alk.	Cl ⁻	SO ₄ ²⁻	Na ⁺	K ⁺	Mg ²⁺	Ca ²⁺	Br ⁻
Bameridj	D7E4	M	3,560,769.6	720,586.2	296	20/01/2013	2.02	20.1	7.86	1.63	10.1	5.79	9.88	0.68	3.92	2.51	
Bameridj	D7E5	M	3,567,891.7	720,586.2	296	19/06	2.07	21.1	8.2	1.96	10.75	3.54	10.88	0.99	2.32	2.51	
Iffri	D1F151	S	3,538,891.7	721,060.5	204	1996	2.67	23.5	7	1.26	10.75	2.71	7.99	0.73	2.32	2.12	
Saïd Ouba	D2F66	S	3,540,257.3	720,085.4	216	1996	2.31	18	8	1.43	11.02	4.73	11.47	0.16	2.07	3.33	
Oglat Larbaâ	D6F64	M	3,566,201.4	729,369.3	177	27/01/2013	2.31	24	7.9	1.41	11.36	6.85	11.59	2.31	1.96	4.58	
El-Bour	D4F94	M	3,536,245.2	722,641.7	100.6	1996	3.05	26.2	7.37	1.61	12.8	6.79	5.15	1.94	1.65	9.13	
Saïd Ouba I	D2F71	S	3,557,412.4	718,272.8	211.9	1996	2.27	24.2	8.2	1.54	13.53	5.72	14.99	0.33	3.28	2.57	
Dediche	D6F61	M	3,487,357.1	717,067.1	173.5	26/01/2013	2.22	22.9	7.74	1.78	14.2	8.41	12.6	0.66	3.38	4.43	
N'Yassa	D6F51	M	3,551,822.5	718,272.8	198	1996	3.15	23.2	7.54	2.38	14.27	6.86	13.1	0.4	3.36	5.43	
Saïd Ouba I	D2F71	S	3,557,412.4	718,272.8	211.9	1996	5.63	25.1	7.34	2.38	14.3	6.86	13.1	0.4	3.36	5.43	0.034
Rouissat III	D3F10	S	3,535,088.1	722,552.1	248	26/01/2013	2.37	18.9	7.98	1.65	15.4	8.64	12.6	1.56	5.79	4.25	
Iffri	D1F151	S	3,538,891.7	721,060.5	216	27/01/2013	2.37	22.9	7.79	1.75	15.4	8.31	13.7	0.22	5.17	4.75	
Saïd Ouba	D2F66	S	3,540,257.3	720,085.4	216	31/01/2013	2.38	24.9	7.91	2.19	16.1	16.1	16.1	0.74	4.93	4.29	
Oglat Larbaâ	D6F64	M	3,566,201.4	729,369.3	177	31/01/2013	2.43	23.7	7.62	2.3	16.3	8.65	13.6	0.71	5.86	4.97	
SAR Mekhadma	D1F91	S	3,536,257.7	717,822.3	221	03/02/2013	2.47	25.8	7.75	3.43	16.3	8.53	16.1	0.68	5.27	4.92	
N'Yassa	D6F51	M	3,551,822.5	720,886.4	198	25/01/2013	2.65	19.9	8.02	2.14	16.8	9.71	15.9	0.35	3.20	2.91	
A Louise	D4F73	S	3,559,233.4	720,085.4	225.5	25/01/2013	3.36	24.7	8.05	1.98	16.8	9.71	15.9	0.35	3.20	2.91	0.033
Charzalet A.H	D6F79	M	3,537,233.4	721,904.6	319	26/01/2013	2.57	24	7.49	1.98	17.4	9.04	13.9	1.99	5.78	5.05	
Am moussa II	D9F70	S	3,598,750.2	720,356.8	119	02/02/2013	2.84	22.5	7.55	3.47	17.4	9.35	16.6	0.62	6.24	4.96	
Am N sara	D6F50	S	3,537,814.1	719,665.1	220.6	02/02/2013	7.52	23.9	7.52	2.37	17.5	8.24	17.3	0.39	3.1	6.46	0.033
Am N sara	D6F50	S	3,559,233.6	716,868.4	255	02/02/2013	2.62	23.8	7.65	2.11	17.7	9.19	15.5	1.13	6.11	4.73	
H.Milhoud	D1F135	S	3,547,557.1	717,067.1	173	03/02/2013	2.76	21.6	7.55	3.32	17.9	9.22	16.5	1.01	6.17	4.91	
El Bour	D6F61	M	3,540,257.3	715,816.0	169	25/01/2013	2.65	19.9	8.02	2.14	17.9	5.28	15.8	1.6	3.84	4.73	
H.Milhoud	D1F135	M	3,547,557.1	717,067.1	173	03/02/2013	2.65	21.6	7.55	3.32	17.9	9.22	16.5	1.01	6.17	4.91	
N'Yassa	D6F51	M	3,551,822.5	718,976.5	198	31/01/2013	3.07	22.9	7.52	2.03	18.4	9.71	17.1	0.45	6.17	4.99	
El Koun	D6F51	S	3,556,256.7	721,639.7	143	31/01/2013	2.97	22.9	8.09	3.52	18.4	9.71	17.1	0.32	6.49	5.14	
El Koun	D6F67	S	3,573,694.1	721,639.7	143	1996	2.5	25	7.6	1.5	18.79	7.17	10.18	3.43	4.97	5.81	
ITAS	D1F150	M	3,536,186.6	717,046.1	93.1	21/01/2013	3.66	23.9	7.54	1.48	18.8	7.07	10.1	3.41	4.94	5.77	
Am moussa V	D9F13	M	3,538,409.2	718,680.2	210.2	08/02/2013	2.39	25.3	7.22	2.28	19.4	9.45	18.8	0.39	3.31	7.61	
El-Bour	D4F94	M	3,536,245.2	722,641.7	100.6	1996	2.3	21.2	7.9	1.58	20.05	7.21	12.09	2.62	5.76	5.17	
Rouissat I	D2F61	M	3,535,816.2	722,641.7	80.4	26/07/2013	2.13	21	8.15	1.35	21.26	11.2	12.6	0.17	5.98	6.01	
El Bour	D3F18	M	3,535,816.2	722,641.7	80.4	26/07/2013	2.13	21	8.15	1.35	21.26	11.2	12.6	0.17	5.98	6.01	
Si. pompage ebott	D5F80	S	3,541,656.9	723,521.9	224.1	04/02/2013	3.28	24.5	7.84	1.86	21.66	11.9	19.9	2.13	7.64	6.28	
Chart Palmerate	D5F77	S	3,538,219.3	725,541.3	242.8	05/02/2013	3.37	24.6	7.53	3.26	22.3	12.1	20.9	1.15	8.25	6.78	
Bour El Hakha	D1F134	M	3,545,233.1	720,391.7	86	05/02/2013	3.4	22.2	7.34	4.13	23.2	12.2	21.2	1.49	8.61	6.01	
Guet Chemia	D2F69	M	3,552,304.9	712,786.3	137.1	03/02/2013	3.54	24.6	7.61	2.24	24.7	12.7	21.1	1.65	8.45	6.47	
Abzatt	D2F69	M	3,552,304.9	712,786.3	137.1	03/02/2013	4.05	28	7.3	2.21	25.9	9.47	25.4	0.57	3.64	7.17	
Frame	D6F62	M	3,570,175.8	717,133.8	167.5	27/01/2013	3.79	24.2	7.95	2.27	25.9	13.5	22.6	0.64	8.91	7.16	
Am Roub	D6F51	M	3,551,822.5	718,976.5	198	25/01/2013	3.79	24.2	7.95	2.27	25.9	13.5	22.6	0.64	8.91	7.16	
N'Yassa El Hou	D6F51	M	3,551,822.5	718,976.5	198	1996	3.15	23.2	7.54	2.38	28.59	8.61	23.14	0.62	4.42	8.01	0.035
H.Milhoud Benyaza	D1F138	M	3,551,192.5	717,042.1	88.9	28/01/2013	3.85	25.2	7.61	2.44	28.4	14.2	28.4	1.66	10.01	7.12	
Am L.aarab	D6F49	M	3,558,822.6	716,799.1	156.5	28/01/2013	3.97	23.7	7.33	2.16	28.9	9.01	23.9	0.53	5	7.72	0.037
H.Milhoud Benyaza	D1F138	M	3,551,192.5	717,042.1	88.9	1996	2.9	22.8	7.5	2.16	28.92	9.03	23.87	0.52	4.99	7.7	
Rouissat	D3F8	M	3,545,470.7	732,837.6	332.4	03/02/2013	4.38	25.4	7.51	1.71	29.8	8.33	22.8	1.23	6.23	6.08	
Rouissat	D3F8	M	3,545,470.7	732,837.6	332.4	1996	6.16	25.3	7.22	1.71	29.81	8.33	22.8	1.23	6.23	6.08	
Am El Arch	D3F36	M	3,544,854.8	723,521.9	133.0	1996	3.6	25.4	7.22	1.71	29.81	8.33	22.8	1.23	6.23	6.08	
Si. pompage ebott	D3F80	S	3,541,656.9	723,521.9	224.1	1996	3.69	25.4	7.67	2.28	42.22	13.53	36.77	1.12	7.43	9.73	

M = Mioplisene aquifer; S = Senonian aquifer

Table 3: Field and analytical data for the Phreatic aquifer.

Locality	Site	Lat.	Long.	Elev.	Date	EC		T	pH	Alk.	Cl ⁻	SO ₄ ²⁻	Na ⁺	/mmolL ⁻¹			
						mS cm ⁻¹	°C							Ca ²⁺	K ⁺	Mg ²⁺	B ⁻
Khezama	P433	3,597,046	719,626	118	20/01/2013	2,09	22,7	9,18	1,56	12,02	7,3	13	0,99	4,34	2,8		
Khezama	P433	3,597,046	719,626	118	1996	2	22,1	8,86	1,46	12	6,87	11,57	0,93	4,4	2,9		
Hassi Mhould	R059	3,547,216	718,358	124	27/01/2013	2,1	23,9	8,15	1,86	13	7,3	12,6	1,25	4,43	3,43	0,024	
Ain Kheir	P106	3,584,761,4	717,604,5	125	1996	4,01	23,79	7,52	1,86	14,15	17,89	15,89	0,61	10,61	7,5		
Hassi Nagri	PLX3				20/01/2013	2,93	23	8,09	2,04	17,77	9,4	16,6	0,93	5,75		0,031	
	LTP 30				1996	4,08	23,73	7,12	5,25	18,21	9,97	24,29	0,41	1,43	8,13		
Maison de culture	PL31	3,537,988	720,114	124	1996	2,31	23,83	8,08	1,46	18,91	7,8	26,05	0,62	2,13			
El Bour	R006	3,547,216	719,421	161	1996	2,96	23,45	7,88	1,27	18,98	7,74	12,41	4,25	5,32	5,31		
Hassi Mhould	R059	3,547,216	718,358	124	1996	2,77	23,45	7,83	3,29	22,1	12,4	34,17	2,59	8,61	5,47		
Oglet Larba	P430	3,567,287,5	750,058,8	139	24/01/2013	4,5	27,5	8,29	4,22	22,6	8,6	28,4	2,21	4,01	3,17		
Maison de culture	PL31	3,537,988	720,114	124	28/01/2013	3,7	22,2	8,23	2,21	20,83	9,366	21,8	2,21	2,21	2,21	0,032	
France El Koum	P401	3,572,830,2	719,211,4	112	20/01/2013	3,44	27,5	7,52	4,22	23,3	13,4	50,56	2,82	8,25	6,28		
Gherbouz	PL15	3,537,962	718,744	134	1996	2,47	23,47	7,72	2,21	23,54	13,97	23,7	1,77	4,18	7,91		
Bour El Hachia	P408	3,544,999,3	719,930,6	110	1996	2,43	23,46	7,75	2,99	24,16	13,23	41,89	0,88	2,34	0,84		
Station d'epuration	PL30	3,538,398	721,404	130	20/01/2013	5,31	23,80	7,39	3,01	24,32	21,22	24,26	2,32	2,23	2,23	0,025	
France Ank Djemel	P422	3,575,339	724,063,3	127	1996	4,7	23,61	7,22	4,39	25,3	9,5	23,7	2,32	4,96	7,46		
Koume Ain Mousssa	PLX2	3,537,324,9	716,428,5	111	20/01/2013	4,1	25,2	7,61	3,03	26,2	10,36	14,83	0,24	9,33	7,56	0,033	
H Chegga	PLX4	3,577,944,8	716,520,7	129	27/01/2013	3,66	24,6	8,1	2,02	25,68	10,6	24	2,29	4,96	6,55		
Hassi Mhould	R058	3,547,329,7	717,253	133	1996	5,3	23,44	7,69	1,34	28,21	17,58	19	2,29	9,09	7,46	0,033	
Koume Ain Mousssa	R057	3,548,943	714,060	141,6	1996	2,62	23,68	7,76	2,84	28,77	14,52	58,74	0,03	11,48	8,57		
Koume Ain Mousssa	PL15	3,533,586	718,419,1	137	1996	4,67	23,87	7,76	1,75	30,87	16,66	24,9	2,03	15,69	4,49	0,033	
Mekranah	PL18	3,537,109,4	721,119	119	20/01/2013	4,67	22,2	7,89	1,78	31,2	15,4	21,3	2,03	11,17	8,37		
Polyclinique Badobes	PL18	3,537,270	714,428,5	111	1996	4,49	23,67	7,58	1,5	31,2	10,08	20,05	0,8	10,55	7,53		
H Chegga	PLX4	3,577,944,8	713,715	117	1996	4,49	23,69	7,62	1,45	31,94	12,83	22,23	0,8	10,55	7,53		
Koume El Gokla	PL16	3,532,463	718,744	134	21/01/2013	4,65	23,3	8,16	1,78	32,4	14,6	18,5	0,8	6,76	7,89		
Gherbouz	PL15	3,537,962	718,744	113	1996	4,77	23,70	7,70	1,55	32,81	12,85	27,7	0,96	9,19	7,57		
Koume El Gokla	PL17	3,531,435	717,353	111	1996	4,65	23,70	7,64	1,48	33,5	11,9	30,18	0,96	6,76	7,57		
Koume Ain Mousssa	R057	3,548,943	720,170	133	26/01/2013	5,7	26,2	8,21	1,96	33,6	12,1	29,2	3,33	5,98	8,17		
Ecole paramedicale	PL52	3,538,478	719,746	114	21/01/2013	5,72	23,71	7,69	1,32	35,01	13,52	37,1	1,92	6,36	8,17		
DSA	PL10	3,537,035	713,298	111	1996	6,08	25	7,72	1,66	35,4	13,8	37,1	1,92	6,36	8,17		
Koume El Gokla	PL17	3,531,435	713,298	111	03/02/2013	5,5	22,5	8,04	1,66	36,3	11,6	37,1	1,92	6,36	8,17		
Koume El Gokla	PL16	3,532,463	713,715	117	03/02/2013	5,8	22,5	8,04	1,66	36,3	11,6	37,1	1,92	6,36	8,17		
Station d'epuration	PL30	3,538,398	730,922	130	31/01/2013	5,29	25,1	7,84	1,66	38,4	14,6	28,5	4,45	6,75	8,37		
Hassi Debeh	P416	3,538,292,9	719,746	106	24/01/2013	5,5	24,6	8,44	2,37	38,6	16,9	22,3	0,89	4,8	21,26		
DSA	PL10	3,537,035	721,404	114	20/01/2013	5,51	25,4	8,44	2,37	38,6	16,9	22,3	0,89	4,8	21,26		
Hospital	LTPSN2	3,538,292,9	720,442,9	114	27/01/2013	6,09	24,5	7,78	1,62	39,7	11,7	36	1,93	9,03	9,21		
PARC SONNACOM	PL28	3,536,077	719,558	132	21/01/2013	6,09	24,5	7,78	1,62	39,7	11,7	36	1,93	9,03	9,21		
Bour El Hachia	P408	3,544,999,3	719,930,6	110	21/01/2013	6,08	24,5	8,13	1,82	42	10,72	30,6	1,86	5,11	8,46		
Koume Ain Mousssa	R056	3,549,933	717,022	128	1996	7,62	23,65	8,07	2,16	42,14	19,1	18,87	1,86	13,39	8,12		
Koume Ain Mousssa	R056	3,549,933	717,022	128	1996	7,62	23,65	8,07	2,16	42,14	19,1	18,87	1,86	13,39	8,12		
Ecole Okba B. Nafaa	PL41	3,538,660	719,831	127	31/01/2013	6,36	24,1	7,68	2,11	44,9	13,2	36,2	1,18	12,49	8,07		

Table 4: Field and analytical data for the Phreatic aquifer (continued).

Locality	Site	Lat.	Long.	Elev.	Date	EC /mS.cm ⁻¹	T /°C	pH	Alk.	Cl ⁻	SO ₄ ²⁻	Na ⁺ /mmol.L ⁻¹	K ⁺	Mg ²⁺	Ca ²⁺
PARC HYDRAULIQUE															
	P419	3,539,494	725,605	132	31/01/2013	7,03	26,4	7,84	2,05	45,1	14,4	41,4	10,78	5,95	6,91
	PL13	3,536,550	720,200	123	21/01/2013	7,22	24,5	7,51	3,24	47,8	14,5	44,4	10,55	6,35	6,59
	Mekhadna	3,536,230	718,708	129	21/01/2013	7,64	27,1	7,94	1,78	48	14,5	42,9	6,56	7,4	7,61
	P506	3,535,238,1	725,075,1	126	04/02/2013	8,32	24,3	8,12	1,71	52,6	14,6	42,8	10,97	7,51	7,83
	Said Oba	3,535,238,1	725,075,1	126	04/02/2013	6,7	23,28	7,46	1,8	54,39	17,58	33,32	4,11	22,16	5,17
	Mekhadna	3,540,433,1	719,661,3	115	27/01/2013	9	24,6	7,64	1,72	62,5	15,2	71,6	4,61	4,08	6,06
	P566	3,536,908	718,511	130	21/01/2013	9,4	24,5	8,06	3,39	63,2	15,6	77,2	2,51	4,08	5,11
	Mekhadna	3,530,116,2	722,775,1	130	04/02/2013	10,09	30,2	7,91	1,63	63,6	21,5	88,3	4,08	4,21	4,65
	Palim, Gara Krima	3,536,230	718,708	129	19/06	9,5	23,72	7,96	0,63	75,57	10,62	10,22	2,64	32,94	9,54
	PL25	3,542,636,5	718,957,4	126	19/06	7,75	23,48	7,62	1,51	80,23	12,45	45,87	2,46	23,59	5,91
	Mekhadna (Bab-shaa)	3,540,010,9	725,738,1	130	19/06	7,34	23,86	7,60	3,04	84,14	30,58	108,55	2,23	10,17	8,99
	CEM Malek B. Nahi	3,536,074	721,268	128	19/06	9,73	23,82	7,25	4,46	84,26	23,68	61,62	3,75	33,53	1,88
	ENTV	3,538,419	720,950	126	19/06	1,5	24,2	8,2	4,53	86,6	16,7	79,9	3,21	14,54	6,85
	Hôtel Transat	3,537,109,4	718,419,1	128	28/01/2013	16,41	25,7	7,45	1,97	99,9	17,4	85,5	5,7	15,66	7,6
	Mekhadna	3,537,109,4	718,419,1	137	21/01/2013	16,8	24,8	7,64	2,02	101,3	17,7	85,9	5,85	16,69	7,59
	PL05	3,537,099,4	721,673,9	134	19/06	4,68	23,85	7,19	2,74	109,75	67,21	134,67	5,71	42,02	8,77
	Beni Thour	3,537,675	719,416	125	22/01/2013	17,08	24,9	8	3,41	114,2	18,1	92,9	12,8	16,85	7,81
	Tazegrant	3,540,010,9	725,738,1	130	03/02/2013	10,84	23,1	7,54	3,29	117,3	14,7	116,4	2,06	8,99	7,24
	PL03	3,564,272	719,421	161	19/06	12,42	23,6	7,71	2,38	131,9	18,1	96,3	8,61	52,44	6,25
	CEM Malek B. Nahi	3,551,711	720,591	103	27/01/2013	18,31	26,4	7,85	4,03	138	16,7	108,8	13,06	19,51	8,72
	El Bour	3,541,410,1	723,501,1	138	19/06	19,01	26,4	7,67	2,68	142,22	24,5	125,9	3,1	27,11	7,99
	Ain Moussa	3,536,039,3	721,673,9	134	28/01/2013	20,18	25,8	7,8	4,96	153	17,7	125,9	3,16	44,22	3,02
	Station de pompage	3,535,474	718,407	126	21/01/2013	21,23	24,8	8,11	1,7	169,4	18,4	130,3	6,29	22,83	8,08
	Drain Chott Ouargla	3,540,137	716,721	118	26/01/2013	22,31	27,2	7,57	4,33	171,5	17,1	130,8	4,89	27,81	8,63
	Beni Thour	3,559,563	716,543	135	26/01/2013	25,94	24,5	8,18	7,95	208,6	13,4	198,9	3,61	18,1	8,83
	CNMC	3,559,388	717,707	123	26/01/2013	27,51	28,4	8,39	11,45	208,8	15,8	195,1	2,65	18,7	9,01
	Bamerdil				19/06	11,53	23,78	7,48	3,84	213,35	48,63	147,9	7,46	75,31	4,25
	PL04				19/06	17,18	23,64	7,59	3,37	235,01	46,44	264,84	4,74	25,57	5,56
	PL44	3,540,758,8	726,115,6	132	28/01/2013	32,93	23,4	7,95	4,44	245,6	20,9	141,4	26,88	44,56	17,66
	Route Adjadja Aven	3,569,043	721,496	134	02/02/2013	31,03	23,5	8,01	6,91	252,7	17,9	208,2	9,41	29,99	10,03
	PLX1	3,562,236	718,651	129	26/01/2013	30,07	28,4	7,76	5,42	254,7	15,5	209,2	10,43	28,82	7,51
	Route Frane	3,537,323,9	724,063,3	127	21/01/2013	43,25	25,7	8,07	5,15	262,2	9,3	270,4	15,5	62,77	21,46
	El Bour-N' gouca	3,551,711	720,591	103	25/01/2013	32,02	22,7	8,03	2,95	263	15,4	206,9	6,56	32,12	9,95
	PLX2	3,549,503	721,514	138	25/01/2013	60	28,7	8,6	7,69	313,2	93,9	442,8	23,26	12,56	10,17
	Route Ain Bida	3,572,148	722,336	127	19/06		23,63	8,37	4	323,62	58,13	331,43	5,01	49,77	3,97
	Ain Moussa	3,551,466	719,339	131	19/06		23,40	7,31	3,98	336,96	64,29	336,67	5,53	62,37	5,45
	Route Frane	3,562,060	717,719	113	02/02/2013	60,58	27,8	7,65	6,02	356,2	96	432,5	29,77	21,02	26,23
	PL04	3,562,122	716,590	110	26/01/2013	61,06	26,2	8,42	6,46	372,4	82,3	347,1	22,64	60,71	26,63
	PL18	3,551,466	719,339	131	25/01/2013	49,04	25,2	7,89	1,8	390,7	21,1	389,3	2,41	18,97	7,39
	Ain Moussa	3,555,586	714,576	105	03/02/2013	62,24	24,8	8,2	5,96	414,8	83,8	362,7	33,34	70,23	26,51
	Route Sedratra	3,559,388	717,707	123	19/06		23,27	7,84	2,4	426,85	57,81	393,83	9,13	59,13	12,02
	PL09														
	N' Goussa														

Table 5: Field and analytical data for the Phreatic aquifer (continued).

Locality	Site	Lat.	Long.	Elev.	Date	EC	T	pH	Alk.	Cl ⁻	SO ₄ ²⁻	NH ₄ ⁺	K ⁺	Mg ²⁺	Ca ²⁺
			/m			/mS cm ⁻¹	/°C					/mmol/L			
Roume France	P001	3.572,148	722,366	127	02/02/2013	66,16	28,3	7,24	6,49	468,7	101,5	350,3	25,96	116,21	35,31
Sekket Salfoume	P031	3.577,804	720,172	120	1996		23,75	7,31	6,32	481,83	43,35	326,82	12,61	94,15	23,56
Sekket Salfoume	P031	3.577,804	720,172	120	02/02/2013	75,96	27,9	8,06	5,85	500,3	110,3	470,5	28,67	79,12	35,47
Roume France	P002	3.570,523	722,028	108	1996		23,81	7,76	6,29	522,39	182,95	653,78	9,97	104,7	10,99
Sekket Salfoume	P030	3.577,253	721,936	130	1996		23,52	7,72	4,43	527,7	123,48	533,79	11,59	106,21	10,65
Oum Karab	P012	3.584,089	718,612	114	25/01/2013	64,05	30,3	7,83	7,77	534,3	20,9	529,6	6,41	19,73	4,73
Oum Karab	P012	3.584,089	718,612	114	1996		23,41	7,46	2,72	539,35	60,64	413,55	5,55	112,77	9,42
ANK Djenel	P423	3.540,881	723,178	102	31/01/2013	90,8	23,5	7,48	6,19	636,5	101,3	495,5	5,89	125,81	30,32
Saïd Ouh-Chout	P006	3.540,265	724,729	111	1996		23,59	7,71	3,69	645,07	78,46	357,28	5,89	208,4	12,86
ANK Djenel	P030	3.577,253	721,936	130	03/02/2013	64,66	23,1	7,83	3,71	671,8	90,3	742,9	15,97	41,46	7,65
N'Graissa	P017	3.573,943	723,161	105	26/01/2013	100,1	31	7,13	3,78	679,3	114,1	597,8	10,71	125,85	26,29
ANK Djenel	P021	3.573,943	723,161	105	1996		23,55	7,43	4,24	700,77	154,45	608,68	53,6	85,85	163,08
Station de pompage	PL04	3.541,410,1	723,501,1	108	02/02/2013	63,82	23,30	7,42	2,37	716,27	34,75	560,07	7,04	77,72	11,04
Roume France	P002	3.570,523	722,028	108	1996		25,9	7,57	1,65	748,5	62,6	615,9	14,72	77,72	27,29
Saïd Ouh-Chout	P006	3.540,265	724,729	111	03/02/2013	68,31	23,0	7,18	1,24	771	53,1	711,46	23,46	69,64	30,59
N'Graissa	P019	3.542,656	717,719	113	1996		23,30	7,72	1,44	779,13	77,13	711,46	9,23	77,72	12,05
Saïd Ouh(Bib-shou)	P006	3.542,656	718,957,4	105	1996		29,6	7,15	2,42	842,8	824	1.240,7	18,95	37,63	18,06
ANK Djenel	P018	3.573,943	723,161	126	24/01/2013	82,28	30,7	7,46	1,24	800,4	94,4	824	49,54	319,35	25,59
N'Graissa	P021	3.546,133	716,590	110	1996		23,29	7,15	2,43	842,8	824	1.309,9	13,3	33,47	17,74
Oum Karab	P162	3.535,586	725,129	98	25/01/2013	160	27,4	7,70	2,81	954,89	124,85	997,52	49,54	319,35	25,59
Roume Sedra	P113	3.547,234	714,576	110	1996		23,66	7,37	2,88	980,1	81	824	13,3	33,47	17,74
Hotel Transit	PZ12	3.547,234	722,931	105	05/02/2013	114,9	23,49	7,44	2,88	980,1	81	824	13,3	33,47	17,74
Oum Karab	PL23	3.538,419	720,950	126	1996		23,49	7,42	2,25	1.103,31	14,7	1.058,21	19,14	270,91	13,3
Sekket Salfoume	P023	3.579,698	725,726	99	05/02/2013	130	29,4	7,82	1,76	1.176,99	91,14	1.058,21	11,72	18,27	12,41
Sekket Salfoume	P023	3.579,698	725,726	99	1996		23,32	7,42	1,85	1.189,1	14,7	1.058,21	11,72	18,27	12,41
Sekket Salfoume	P034	3.577,198	725,726	97	05/02/2013	117,9	23,60	7,64	1,94	1.209,3	15,6	1.129,4	8,38	42,85	10,15
Chert Adiafja	PLX1	3.540,758,8	726,115,6	132	1996		23,77	7,67	1,85	1.209,3	15,6	1.129,4	8,38	42,85	10,15
Sekket Salfoume	P063	3.545,586,8	725,667,4	99	1996		23,26	7,71	1,41	1.379,35	139,61	1.257,42	41,55	190,51	10,03
Bamerndi	LT06	3.540,137	716,721	118	1996		23,53	7,71	1,41	1.638,66	143,36	1.321,87	26,85	331,38	12,26
El Boue-N'poca	P076	3.542,236	718,651	129	05/02/2013	178,9	23,26	7,67	1,43	1.860,53	91,55	1.434,73	26,2	278,77	13,25
Sekket Salfoume	P063	3.545,586,8	725,667,4	99	1996		23,39	7,79	1,43	1.887,9	92,9	1.455,8	26,66	282,88	13,44
P068	P004				05/02/2013		23,42	7,49	1,49	2.106,07	182,7	1.765,47	27,33	171,23	6,54
P042	P003				1996		23,42	7,59	1,49	2.106,07	182,7	1.765,47	27,33	171,23	6,54
P068	P006				1996		23,42	7,59	1,49	2.106,07	182,7	1.765,47	27,33	171,23	6,54
PZ12	P046	3.547,234	722,931	110	1996		23,31	7,54	3,35	2.330,85	101,22	1.963,71	52,19	248,1	11,44
Hasri Dehch	P416	3.581,097	730,922	106	1996		23,33	7,84	2,21	2.335,67	222,08	2.302,25	26,84	219,9	7,19
N'Graissa	P041	3.559,563	716,543	135	1996		23,38	7,94	4,33	2.405,55	109,92	2.178,55	25,23	199,35	12,65
Sekket Salfoume	P034	3.579,698	725,633	97	1996		23,37	7,85	1,95	2.433,73	178,87	2.361,09	24,34	196,07	9,2
P039	P039				1996		23,34	7,85	1,95	2.433,73	178,87	2.361,09	24,34	196,07	9,2
P074	P074				1996		23,54	6,87	4,17	2.752	324,58	2.878,99	44,57	152,83	10,97
Sekket Salfoume	P036				1996		23,36	6,92	1,52	4.189,51	201,44	2.616,77	17,9	180,14	9,23
Sekket Salfoume	P036				1996		23,35	7,54	1,4	4.356,48	184,54	4.042,62	2,9	257,81	22,63
Sekket Salfoume	P036				1996		23,35	7,54	1,4	4.356,48	184,54	4.042,62	2,9	257,81	22,63
Sekket Salfoume	P036				1996		23,35	7,54	1,4	4.972,75	108,12	4.692,23	36,84	221,13	9,63

Table 6: Isotopic data ^{18}O and ^3H and chloride concentration in Continental Intercalaire, Complexe Terminal and Phreatic aquifers (sampling campaign in 1992).

Phreatic aquifer											
Piezometer	Cl^- /mmolL $^{-1}$	$\delta^{18}\text{O}$ /‰	^3H /UT	Piezometer	Cl^- /mmolL $^{-1}$	$\delta^{18}\text{O}$ /‰	^3H /UT	Piezometer	Cl^- /mmolL $^{-1}$	$\delta^{18}\text{O}$ /‰	^3H /UT
P007	1.860.5	-2.49	0	PL15	23.54	-7.85	0.6(1)	P074	4.356.4	3.42	6.8(8)
P009	426.85	-6.6	1.2(3)	P066	80.23	-8.14	0.8(1)	PL06	14.15	-8.13	1.0(2)
P506	54.39	-6.83	1.6(3)	PL23	1,103.32	-6.1	0	PL30	24.32	-7.48	2.4(4)
P018	818.67	-2.95	6.2(11)	P063	1,379.3	-3.4	8.7(15)	P002	522.39	-5.71	0.6(1)
P019	779.13	-4.67	5.6(9)	P068	2,335.6	-3.04	8.8(14)	PL21	84.26	-7.65	1.2(2)
PZ12	2,405.5	-2.31	8.1(13)	P030	527.7	-6.57	2.4(4)	PL31	18.91	-7.38	1.6(3)
P023	1,176.9	-2.62	0.2(1)	P076	1,743.5	-5.56	2.8(5)	P433	12	-8.84	0
P416	2,433.7	-7.88	5.9(9)	P021	700.7	-5.16	2.6(4)	PL03	84.14	-7.35	1.7(3)
P034	2,752	-1.77	5.7(9)	PL04	716.27	-2.89		PL44	109.75	-8.82	1.0(2)
P036	4,972.7	3.33	2.1(4)	P093	2,198.5	-2.64	5.1(8)	PL05	30.87	-7.44	1.9(3)
P037	4,953.8	3.12	1.8(3)	P096	645.07	-6.13	4.8(8)	P408	24.16	-7.92	0
P039	4,189.5	0.97	2.2(4)	PLX1	1,296.6	-5.6	1.1(2)	PL16	31.94	-7.18	1.1(2)
P041	2,599.7	-0.58	7.3(13)	PLX2	25.68	-7.6	1.3(2)	LTP 16	213.35	-7.48	1.6(3)
P044	2,106.1	-4.46	2.7(5)	P015	134.68	-6.77	3.0(5)	PL17	32.81	-6.92	0.1
P014	336.96	-6.9	2.8(5)	P001	323.62	-4.66	2.5(4)	PL10	35.01	-7.31	0.2(1)
P012	539.3	-6.41	2.2(4)	P100	235.01	-5.81	0	PL25	75.57	-7.41	0.9(2)
P042	2,330.8	2.05	6.0(10)	P056	42.14	-7.03	2.9(5)	LTP30	18.21	-7.5	1.1(2)
P006	18.98	-6.64	0.5(1)	P113	954.89	-4.75	0.8(2)	LTP06	1,638.6	-1.97	2.8(5)
P057	28.21	-7.33	1.1(2)	PLX4	31.52	-7.1	0.3(1)	P031	481.83	-6.06	3.0(5)
P059	20.83	-7.81	0	P115	28.77	-2.54	6.8(12)				

Complexe Terminal aquifer											
Borehole	Cl^- /mmolL $^{-1}$	$\delta^{18}\text{O}$ /‰	^3H /UT	Borehole	Cl^- /mmolL $^{-1}$	$\delta^{18}\text{O}$ /‰	^3H /UT	Borehole	Cl^- /mmolL $^{-1}$	$\delta^{18}\text{O}$ /‰	^3H /UT
D5F80	42.22	-7.85		D1F138	28.92	-8.13	0.7(1)	D2F71	13.53	-8.23	0.6(1)
D3F8	29.81	-8.14	1.4(2)	D3F18	21.66	-8.23	0.2(1)	D7F4	10.6	-8.27	0.1(1)
D3F26	34.68	-7.97	0.8(1)	D3F10	14.27	-7.88	1.5(2)	D2F66	11.02	-8.3	
D4F94	20.05	-8.18	0.6(1)	D6F51	28.39	-7.9	0.7(1)	D1F151	10.75	-8.32	0.4(1)
D6F67	18.79	-8.23	3.7(6)	D1F135	18.08	-7.97	1.1(2)	D6F64	11.36	-8.28	4.3(7)

Continental Intercalaire aquifer											
Borehole	Cl^- /mmolL $^{-1}$	$\delta^{18}\text{O}$ /‰	^3H /UT	Borehole	Cl^- /mmolL $^{-1}$	$\delta^{18}\text{O}$ /‰	^3H /UT	Borehole	Cl^- /mmolL $^{-1}$	$\delta^{18}\text{O}$ /‰	^3H /UT
Hadeb I	5.8	-8.02	0	Hadeb II	6.19	-7.93	0.1(1)	Aouinet Moussa	6.49	-7.88	1.1(2)

Table 7: Statistical parameters for Continental Intercalaire (CI), Complexe Terminal (CT) and Phreatic (Phr) aquifers samples selected on the basis of $\delta^{18}\text{O}$ and Cl^- data (see text).

Aquifer	Size	Parameter	EC /mS cm $^{-1}$	T /°C	pH	Alk.	Cl^-	SO_4^{2-}	Na^+	K^+	Mg^{2+}	Ca^{2+}
CI	11	Average	2.2	49.0	7.5	2.3	11.0	4.7	10.3	0.51	3.6	2.4
CI	11	Stdd. dev.	0.3	2.0	0.2	1.0	4.6	2.5	4.6	0.23	2.0	1.8
CT	50	Average	3.2	23.0	7.8	2.3	20.0	8.9	17.0	1.0	5.5	5.6
CT	50	Stdd. dev.	1.1	2.4	0.4	0.8	7.0	2.6	6.0	0.8	2.2	1.7
Phr pole I	30	Average	3.9	24.0	7.9	2.3	24.7	11.8	24.2	2.1	7.2	5.3
Phr pole I	30	Stdd. dev.	1.3	1.3	0.4	1.0	6.9	3.4	11.0	1.7	5.0	2.7
Phr pole II	3	Average		23.4	7.0	2.4	4,761.0	158.0	4,021.0	32.4	500.0	13.0
Phr pole II	3	Stdd. dev.		0.1	0.5	1.6	350.0	43.0	1,093.0	28.0	378.0	8.0

Table 8: Summary of mass transfer for geochemical inverse modeling. Phases and thermodynamic database are from Phreeqc 3.0 (Parkhurst and Appelo, 2013).

Phases	Stoichiometry	CI/CT	CT/Phr I	Rainwater/P036	PhrI/PhrII 60%/40%
Calcite	CaCO ₃	—	-6.62×10^{-6}	-1.88×10^{-1}	-2.26×10^{-1}
CO ₂ (g)	CO ₂	-6.88×10^{-5}	—	8.42×10^{-4}	5.77×10^{-4}
Gypsum	CaSO ₄ · 2 H ₂ O	4.33×10^{-3}	—	1.55×10^{-1}	1.67×10^{-1}
Halite	NaCl	7.05×10^{-3}	3.76×10^{-3}	6.72	1.28
Sylvite	KCl	2.18×10^{-3}	1.08×10^{-3}	4.02×10^{-1}	—
Bloedite	Na ₂ Mg(SO ₄) ₂ · 4 H ₂ O	—	1.44×10^{-3}	—	—
Huntite	CaMg ₃ (CO ₃) ₄	—	—	4.74×10^{-2}	5.65×10^{-2}
Ca ion exchange	CaX ₂	-1.11×10^{-3}	—	—	—
Mg ion exchange	MgX ₂	1.96×10^{-3}	—	1.75×10^{-1}	-2.02×10^{-1}
Na ion exchange	NaX	—	—	—	3.92×10^{-1}
K ion exchange	KX	-1.69×10^{-3}	—	-3.49×10^{-1}	1.20×10^{-2}

Values are in mol/kg (H₂O). Positive (mass entering solution) and negative (mass leaving solution) phase mole transfers indicate dissolution and precipitation, respectively; — indicates no mass transfer.

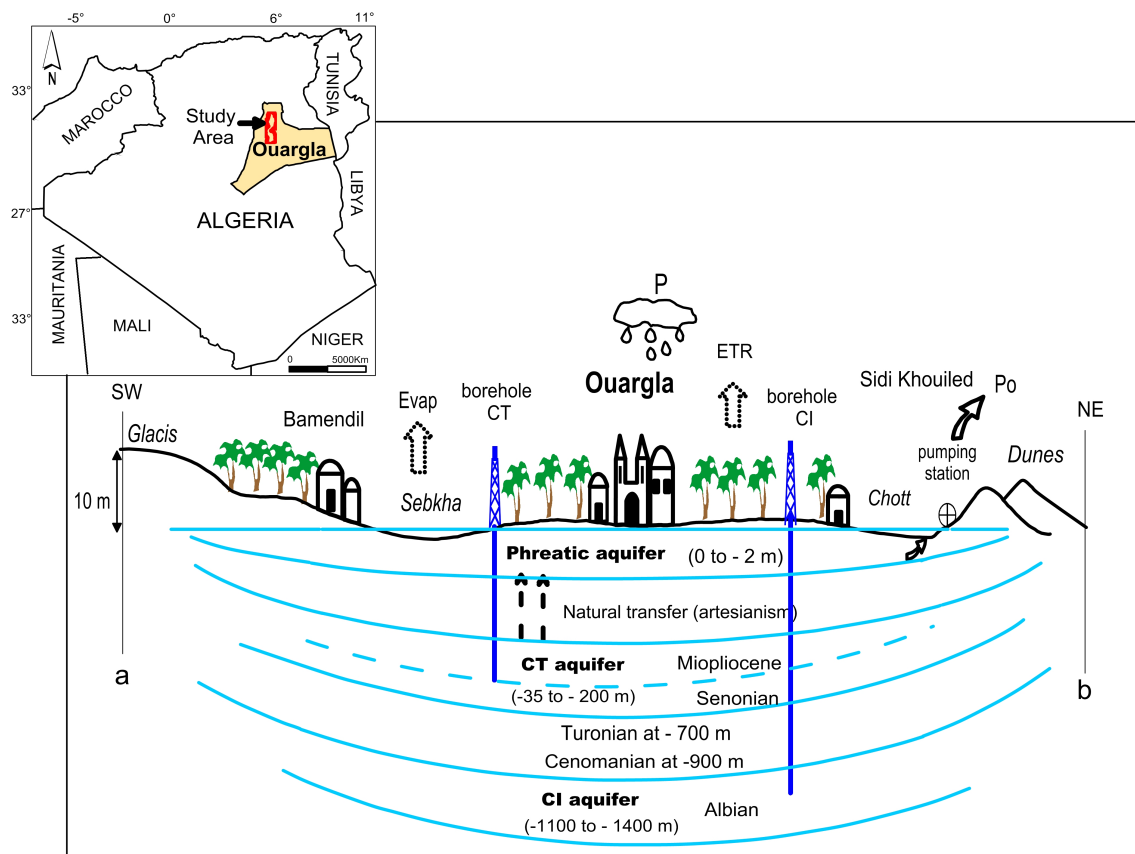


Figure 1: Localisation and schematic relations of aquifers in Ouargla. *Blue lines represent limits between aquifers, and the names of aquifers are given in bold letters; as the limit between Senonian and Miopliocene aquifers is not well defined, a dashed blue line is used. Names of villages and cities are given in roman (Bamendil, Ouargla, Sidi Khouiled), while geological/geomorphological features are in italic (Glacis, Sebkh, Chott, Dunes). Depths are relative to the ground surface. Letters a and b refer to the cross section (fig. 2) and to the localisation map (fig. 3).*

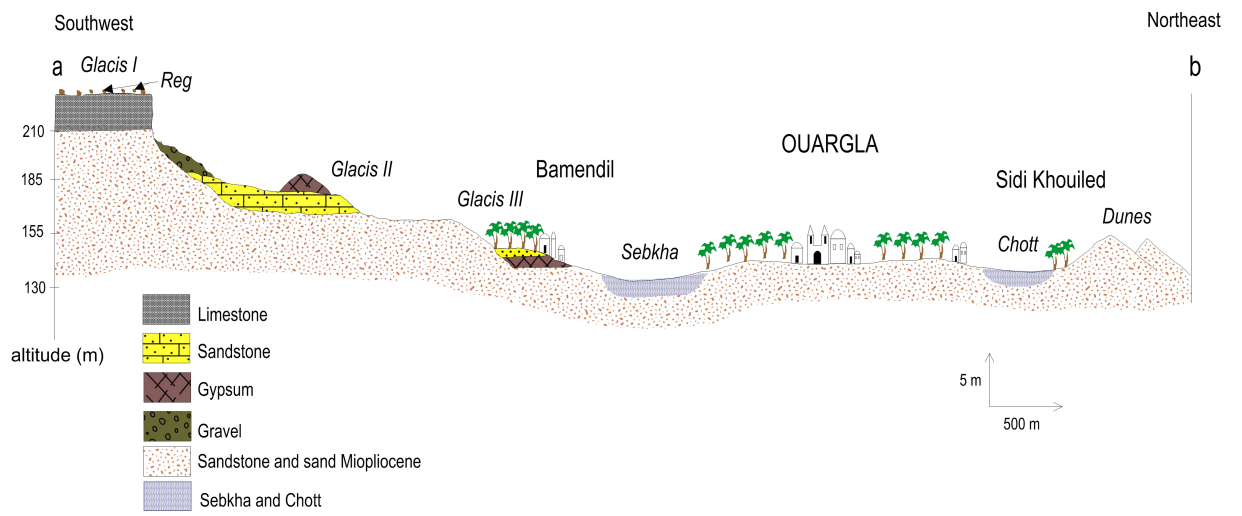


Figure 2: Geologic cross section in the region of Ouargla.
The blue pattern used for Chott and Sebkha correspond to the limit of the saturated zone.

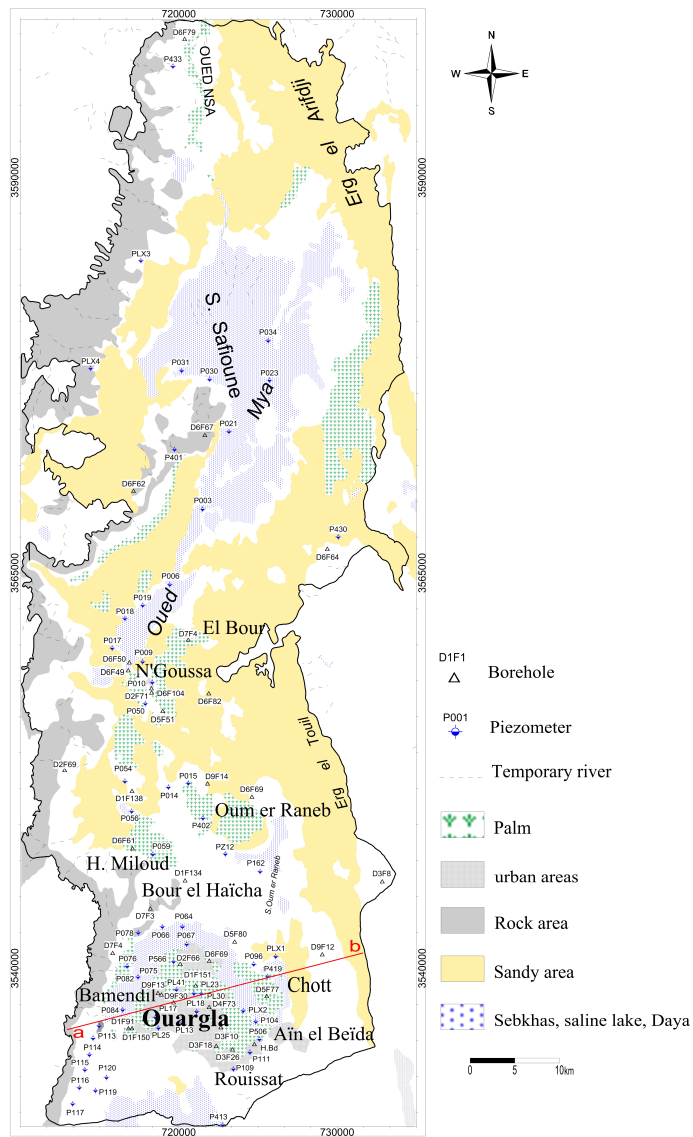


Figure 3: Localisation map of sampling point

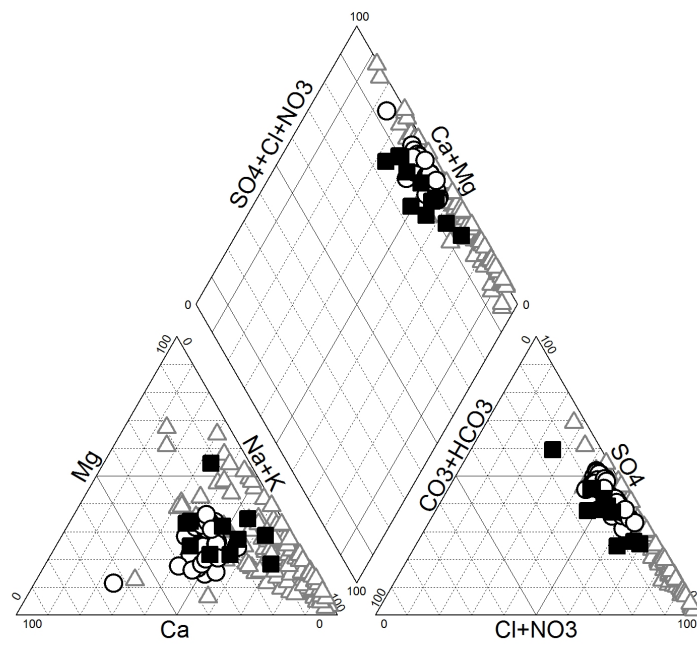
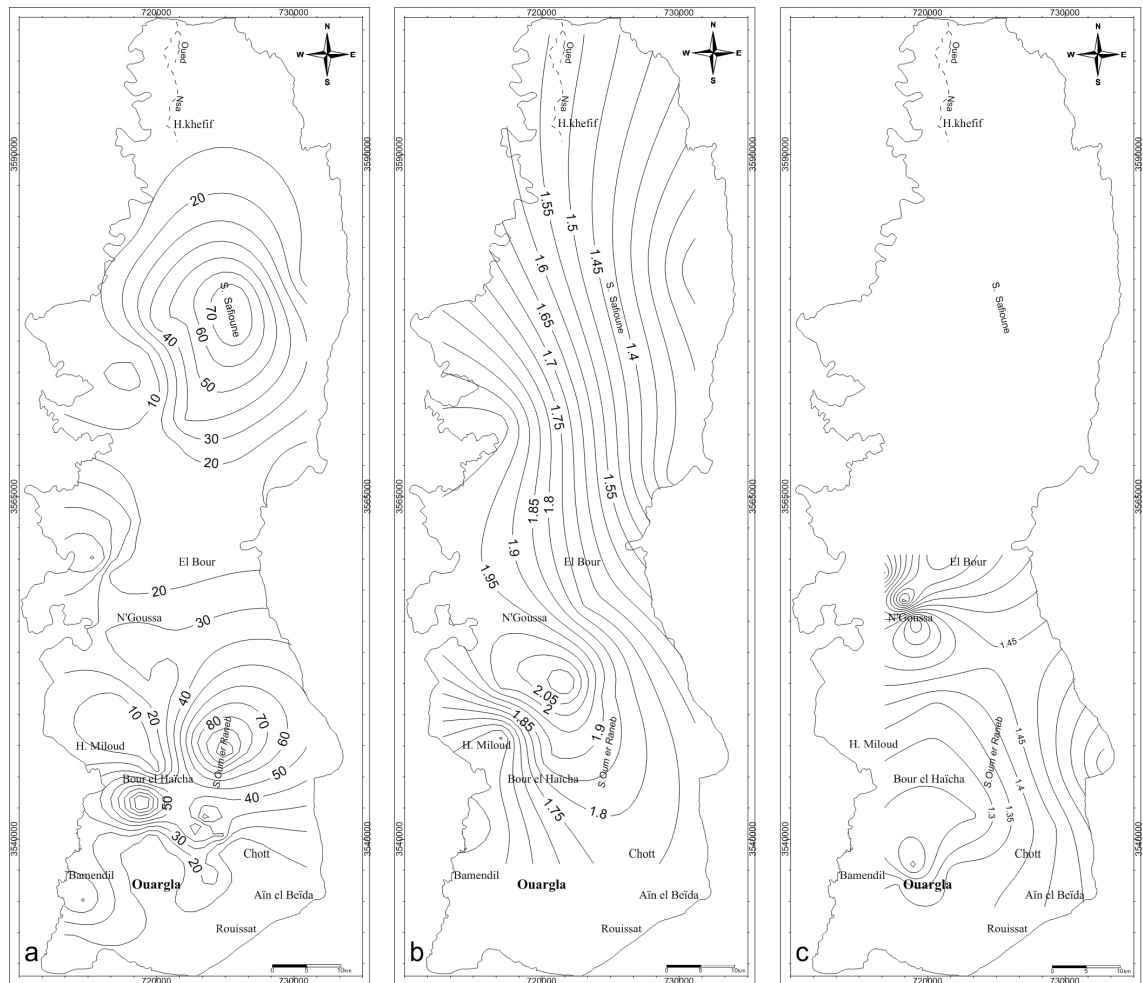


Figure 4: Piper diagram for Continental Intercalaire (filled squares), Complexe Terminal (open circles) and Phreatic aquifer (open triangles).



5

Figure 5: Contour maps of the salinity (expressed as global mineralization) in the aquifer system, (a) Phreatic aquifer; (b) and (c) Complexe Terminal [(b) Miopliocene and (c) Senonian]; figures are isovalues of global mineralization (values in g/L).

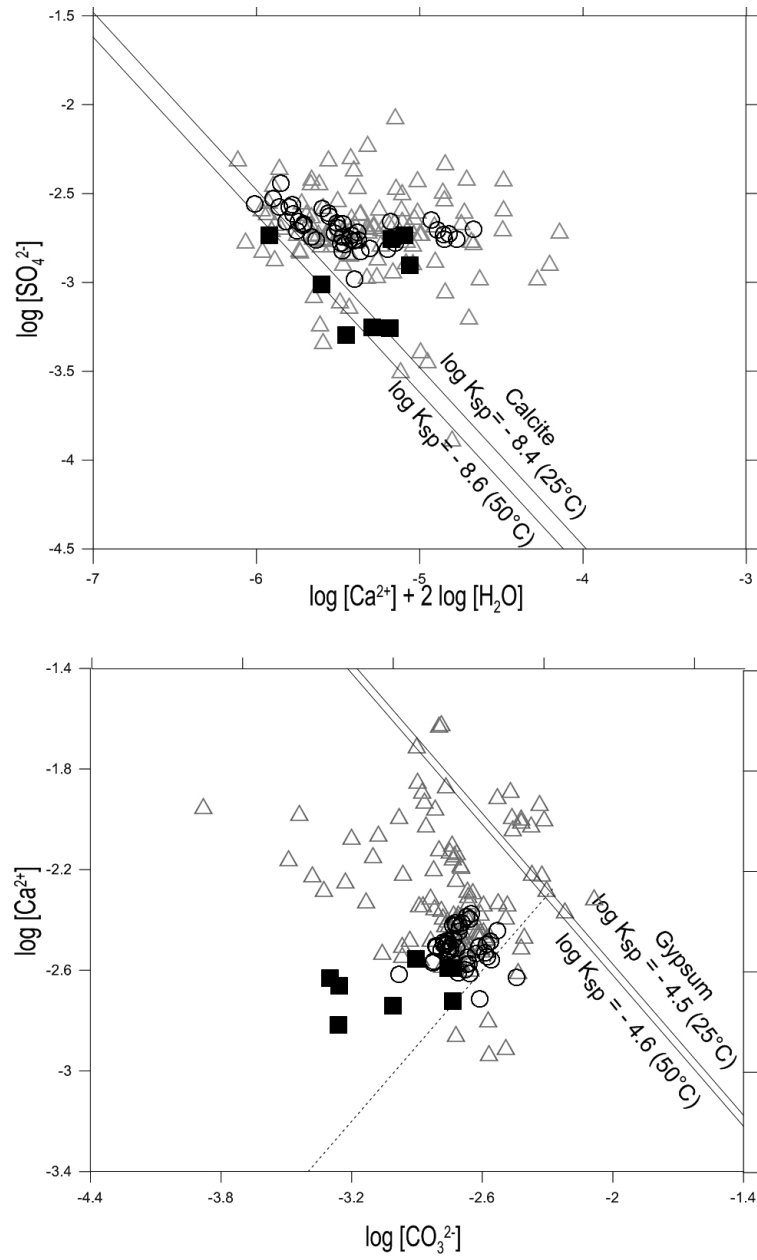


Figure 6: Equilibrium diagrams of calcite (top) and gypsum (bottom) for Continental Intercalaire (filled squares), Complexe Terminal (open circles) and Phreatic aquifer (open triangles). Equilibrium lines are defined as: $\log[\text{Ca}^{2+}] + \log[\text{CO}_3^{2-}] = \log K_{sp}$ for calcite, and $\log[\text{Ca}^{2+}] + 2 \log[\text{H}_2\text{O}] + \log[\text{SO}_4^{2-}] = \log K_{sp}$ for gypsum.

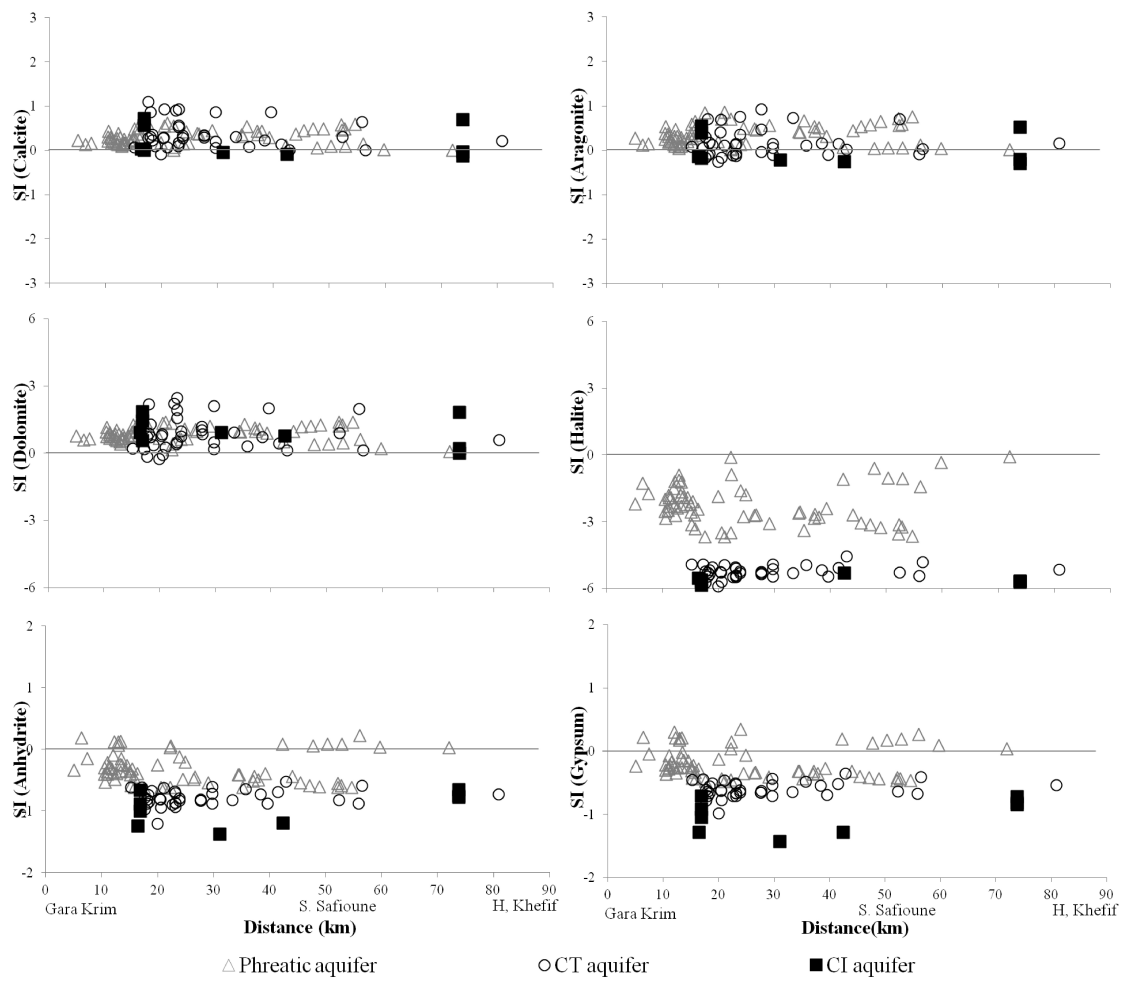


Figure 7: Variation of saturation indices with distance from south to north in the region of Ouargla.

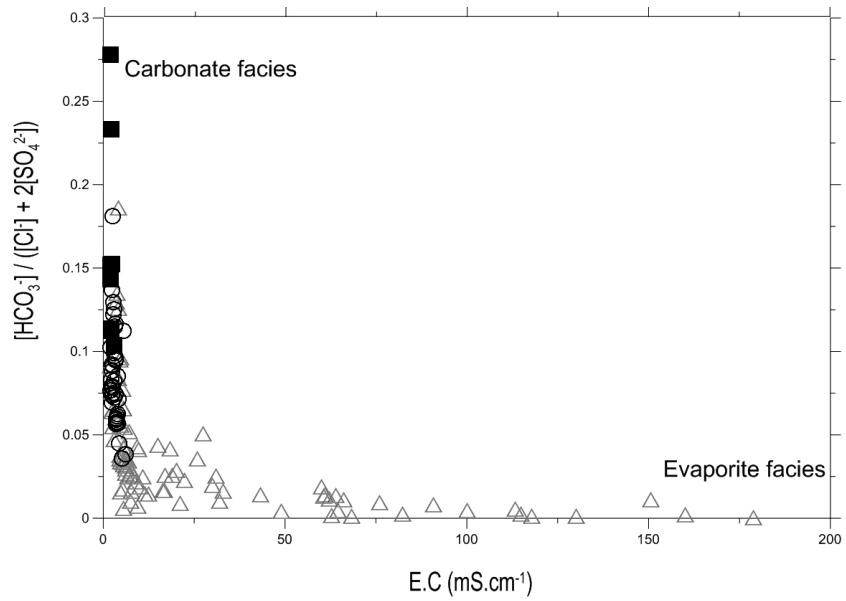


Figure 8: Change from carbonate facies to evaporite from Continental Intercalaire (filled squares), Complexe Terminal (open circles) and Phreatic aquifer (open triangles).

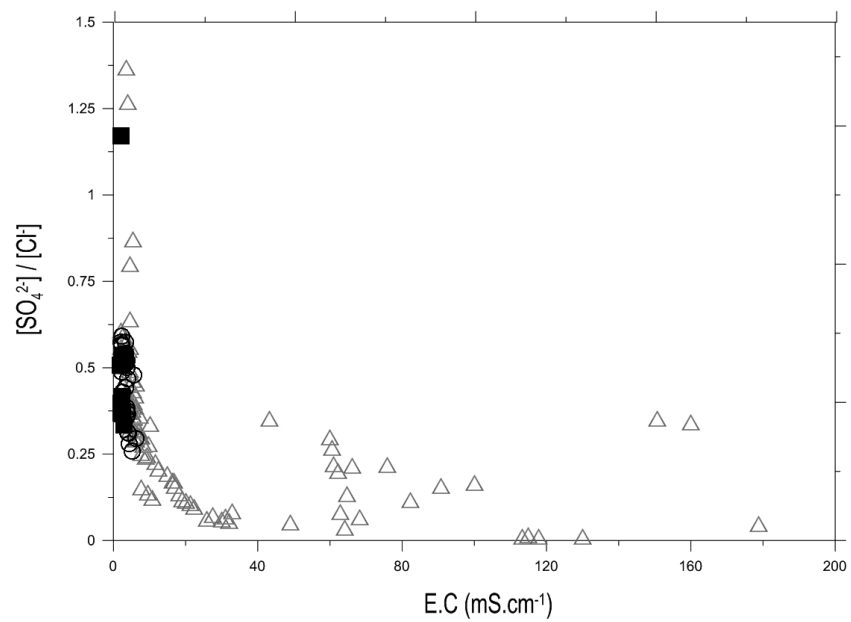


Figure 9: Change from sulfate facies to chloride from Continental Intercalaire (filled squares), Complexe Terminal (open circles) and Phreatic aquifer (open triangles).

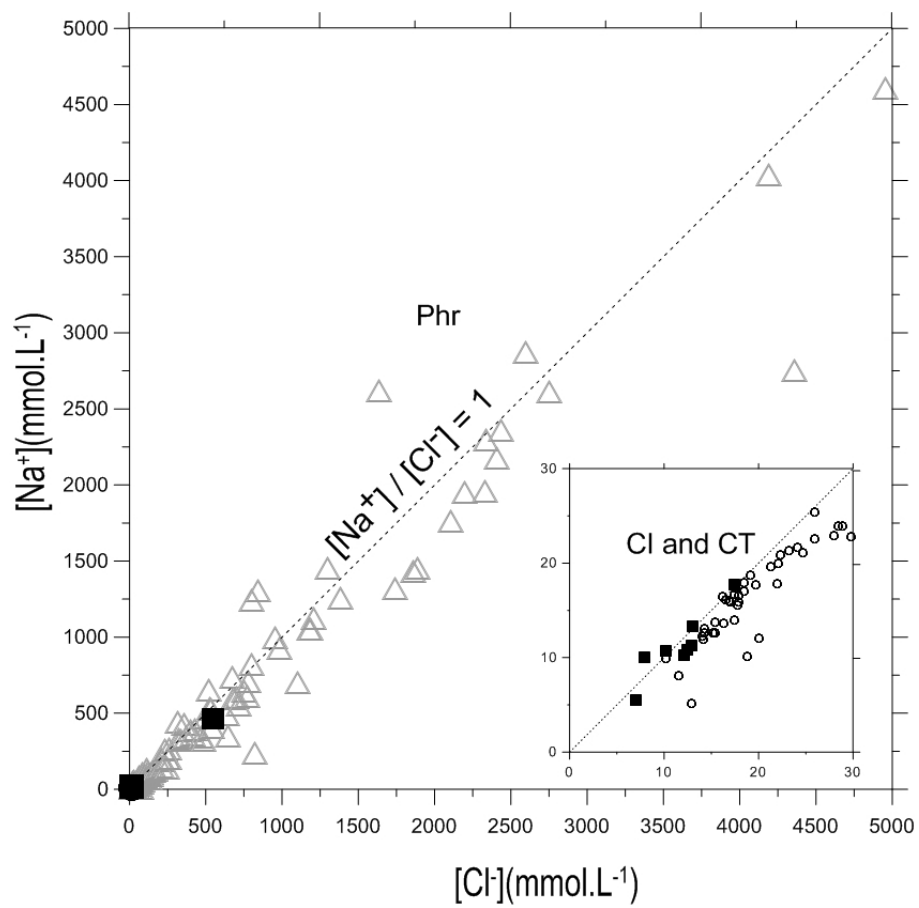


Figure 10: Correlation between Na^+ and Cl^- concentrations in Continental Intercalaire (filled squares), Complexe Terminal (open circles) and Phreatic aquifer (open triangles). Seawater composition (star) is $[\text{Na}^+] = 459.3 \text{ mmol L}^{-1}$ and $[\text{Cl}^-] = 535.3 \text{ mmol L}^{-1}$ (Stumm and Morgan, 1999, p.899).

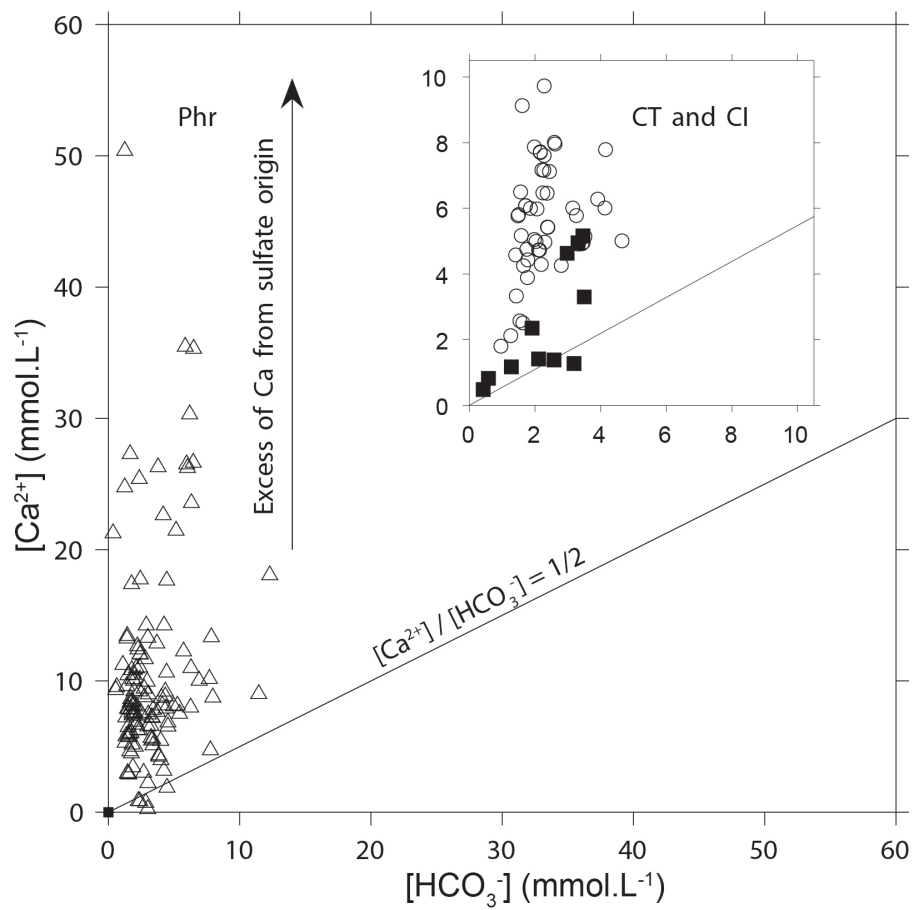


Figure 11: Calcium vs. HCO_3^- diagram in Continental Intercalaire (filled squares), Complexe Terminal (open circles), Phreatic aquifer (open triangles) and Seawater composition (star) is $[Ca^{2+}] = 10.2 \text{ mmol.L}^{-1}$ and $[HCO_3^-] = 2.38 \text{ mmol.L}^{-1}$ (Stumm and Morgan, 1999, p.899).

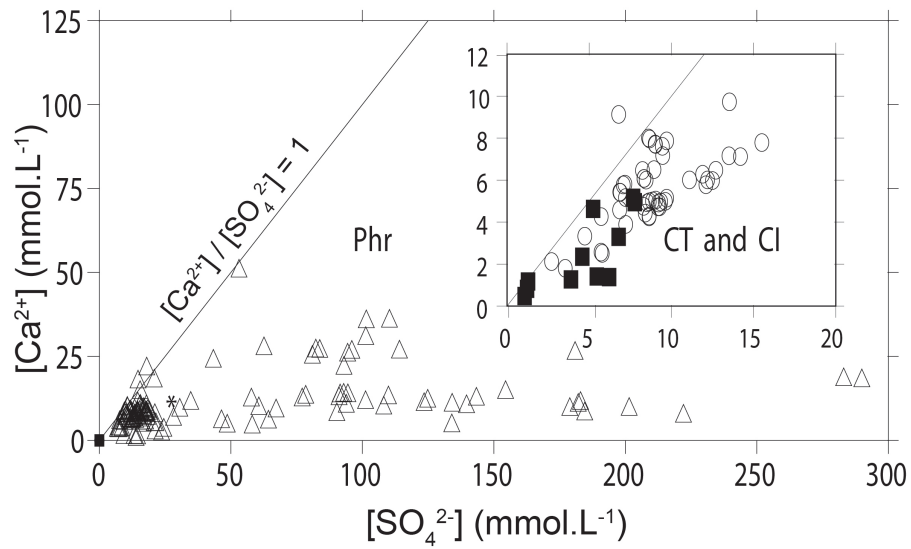


Figure 12: Calcium vs. SO_4^{2-} diagram in Continental Intercalaire (filled squares), Complexe Terminal (open circles), Phreatic aquifer (open triangles) and Seawater composition (star) is $[\text{Ca}^{2+}] = 10.2 \text{ mmol L}^{-1}$ and $[\text{SO}_4^{2-}] = 28.2 \text{ mmol L}^{-1}$ (Stumm and Morgan, 1999, p.899).

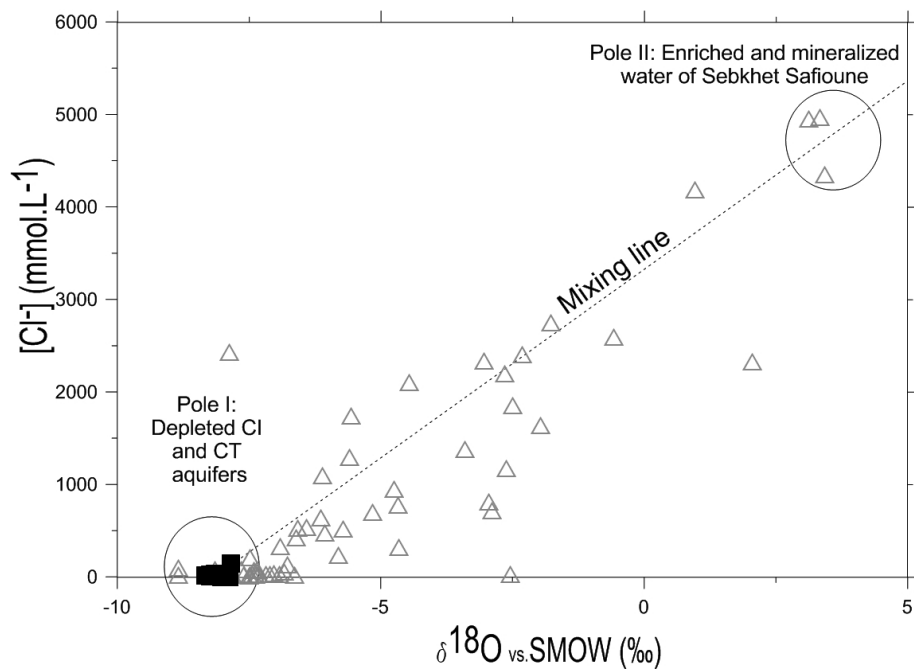


Figure 13: Chloride concentration versus $\delta^{18}\text{O}$ in Continental Intercalaire (filled squares), Complexe Terminal (open circles) and Phreatic aquifer (open triangles) from Ouargla.

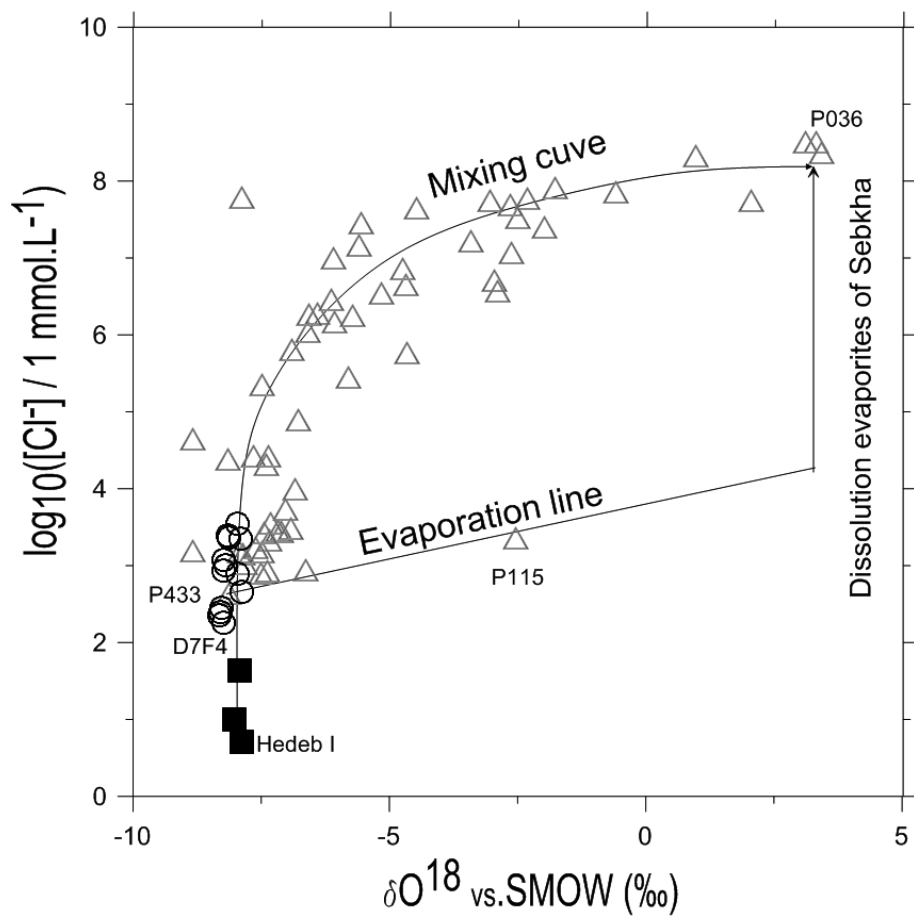


Figure 14: Log $[\text{Cl}^-]$ concentration versus $\delta^{18}\text{O}$ in Continental Intercalaire (filled squares), Complexe Terminal (open circles) and Phreatic aquifer (open triangles) from Ouargla.